Thesis for the Degree of Doctor of Philosophy

The Decoupling Control of Capacity and Superheat for a Variable Speed Refrigeration System

By

Li Hua

Department of Refrigeration and Air-conditioning Engineering

The Graduate School

Pukyong National University

August 2008

The Decoupling Control of Capacity and Superheat for a Variable Speed Refrigeration System

가변속 냉동시스템의 용량 및 과열도의 비간섭 제어

Advisor: Prof. Seok-Kwon Jeong

By

Li Hua

A thesis submitted in partial fulfillment of the requirements

for the degree of

Doctor of Philosophy

In Department of Refrigeration and Air-conditioning Engineering, The Graduate School, Pukyong National University

August 2008

The Decoupling Control of Capacity and Superheat for a Variable Speed Refrigeration System

A dissertation

by

Li Hua

Approved by:

Jung-In Yoon

(Chairman)

Jong-Soo Kum **Jong-Soo Kim**

(Member) **(Member)**

Sam-Sang You **Seok-Kwon Jeong**

(Member) **(Member)**

August 20, 2008

Contents

가변속 냉동시스템의 용량 및 과열도의 비간섭 제어

이 화

부경대학교 대학원 냉동공조공학과

요 약

산업기술의 발전과 쾌적한 주거환경에 대한 요구가 급증하면서 에너지 절약을 위한 인버터 냉동 · 공조시스템이 보편화 되고 있다. 따라서, 장치에 대한 고성능, 고정도의 제어가 필수적으로 요구되고 있다. 그러나 냉동 · 공조시스템의 기본 구성인 냉동사이클은 압축기, 팽창기와 열교환기로 구성되고 이들은 배관을 통해 상호 영향을 미치는 간섭계를 이루고 있을 뿐만 아니라 시스템이 갖는 비선형성으로 인해 명확한 동특성 파악이 어려우며 따라서 제어기의 체계적인 설계가 어렵다.

냉동시스템의 기존 제어법으로는 부하 변동에 따른 에너지 절약을 위한 용량제어와 COP 향상을 위한 증발기의 과열도제어가 주된 핵심이다. 냉동시스템은 그 특성상 압축기 회전수 변화와 전자팽창밸브 개도 변화가 과열도와 실온에 각각 영향을 미치기 때문에 용량제어와 과열도제어를 동시에 독립적으로 제어하기 어렵다. .

용량제어와 과열도제어를 동시에 독립적으로 실행하기 위해 본 연구에서는 실험적인 방법으로 상호 간섭 루프를 배제할 수 있는 비간섭(Decoupling) 모델을 우선 제안하였다. 제안된 비간섭 모델을 이용하여 PI 제어기를 설계하였고, 설계된 PI 제어기를 이용하여 실험을 통해 제안한 방식의 효용성을 입증하였다. 실험결과로부터 제안한 비간섭 모델은 상호 간섭루프를 배제하였기 때문에 제어기의 체계적인 설계가 가능하며 간섭루프를 갖는 PI 제어에 비해 양호한 과도특성을 얻을 수 있을 뿐만 아니라 매우 안정적인 정상상태 특성을 얻을 수 있었다.

또한, 가변속 냉동시스템이 갖는 비선형성과 동특성 모델 구축의 어려움을 고려하여 AI 수법에 의한 퍼지 추론에 근거한 퍼지제어법 적용을 시도해 보았다. 퍼지제어기 설계 시 가변속 냉동시스템에 대한 설계자의 경험을 바탕으로 룰 베이스를 설계하였고, 설계된 제어기를 이용하여 실험을 통해 제어기의 성능을 검토하였다. 퍼지제어기의 제어 성능을 높이

기 위해 본 연구에서는 보상기를 갖는 퍼지제어법도 제안하였다.

본 논문에서 제안한 비간섭 모델과 PI 제어기를 이용한 비간섭 제어법은 가변속 냉동시스템을 고성능, 고정도로 제어하면서 COP 향상과 에너지 절약을 동시에 달성할 수 있는 방법이다. 또한, 제안한 보상기를 갖는 퍼지제어법을 이용한 퍼지제어기도 가변속 냉동시스템의 고성능 제어, COP 향상 및 에너지 절약의 목적을 달성할 수 있다. 따라서 본 연구에서 제안한 설계법은 향후 냉동사이클의 고성능, 고효율 제어에 크게 기여할 것으로 기대된다.

List of tables

List of figures

List of photograph

Nomenclature

b_i	Center of area of a membership function	
C_i	PI controller	
d	disturbance	
e	error in time domain	
ee	the rate of ‘e’	
E	error in complex domain	
f	compressor frequency	[㎐]
G_i	transfer function	
k_i	DC gain	
K_{cr}	critical gain	
K_i	integral gain	
K_p	proportional gain	
L_i	dead time	[s]
P_{cr}	critical period	
Q	thermal load	[㎾]
s	complex Laplace variable	
SH	evaporator superheat	[℃]
SH^*	control reference of superheat	[℃]
t	time	[s]
T_a	chamber temperature	[℃]
T_a^*	control reference of chamber temperature	[℃]

T_{ei}	inlet refrigerant temperature of evaporator	[℃]
T_{eo}	outlet refrigerant temperature of evaporator	[℃]
T_i	integral time	[s]
u	output of PI controller	
U^{crisp}	crisp output of fuzzy inference	
VO	opening angle of EEV	[%]
Δ	variation	
μ_i	output of fuzzy inference	

Chapter 1

Introduction

1.1 Background and objective of this study

With the improvement of standard of living, refrigeration and air conditioning system have been applied widely. A control system must be designed in order to keep indoor temperature within a very restricted range and to reduce energy consumption. It is found that the conventional control schemes in the refrigeration system are primarily focused on two control variables; the degree of superheat and the indoor temperature. In order to improve coefficient of performance (COP), the degree of superheat is maintained at a constant level by adjusting opening angles of expansion valve. The degree of superheat is mainly controlled by a thermostatic expansion valve(TEV) which could regulate evaporating pressure and refrigerant mass flow rate as well in the constant speed refrigeration system. The control capability is highly desirable so as to effectively respond to partial loading conditions for the purpose of maximum possible energy saving. The refrigeration machines are usually operating under the partial loading conditions, generally exploiting conventional on/off-controls for the compressor to keep the indoor temperature within a restricted range with minimum oscillation. However, it is known that the use of such technique coping with partial loadings can deteriorate compressor durability to a considerable extent. Therefore, the on/off control scheme is gradually being replaced by a variable speed refrigeration system(VSRS) with an inverter driven compressor over recent decades. The appearance of the VSRS, the TEV is limited to a very narrow range of mass flow conditions and the superheat is no longer optimum for a wide range of operating conditions. Hence, the electronic expansion valve(EEV) has been used to cope with superheat under severe load variations, instead of TEV[1~2].

The considerable attention has been given to the applications of inverter

refrigeration systems for commercial and residential purposes because of their ability to save energy, while providing better degree of comfort. It is often necessary to design a practical control system in order to control the variable speed refrigeration system(VSRS) for saving energy and guaranteeing high efficiency. The control variables of VSRS are mainly focused on the superheat and the refrigeration capacity. The control method of superheat is adjusting the opening angle of EEV to maintain the superheat at a constant level. And the method of refrigeration capacity control is consisted in varying the compressor speed to continuously match the compressor refrigeration capacity to the thermal load[3~4], In fact, there exist several drawbacks in case of traditionally designed controllers for such a system. It is known that a basic refrigeration cycle consists of a compressor, heat exchangers, and expansions valve. In fact, since all such components in the cycle are connected with various pipes and valves, they show inherent nonlinear characteristics in operational ranges. Hence, it is almost impossible to identify exact dynamic characteristics and develop complete dynamic model for the refrigeration systems. In the VSRS, not only the chamber temperature but also the superheat is changed with the variation of compressor frequency. It is the same as the case of the variation of EEV's opening angle[5~7]. Hence, many studies focused on controlling the superheat or capacity and little of them studied up controlling both of them at the same time[8~15]. It is noted that in the VSRS, the capacity and superheat can not be controlled independently because of interfering loops when the compressor speed and electronic expansion valve opening angle are varied simultaneously.

The objective of this research is divided into three parts: The first objective of this research is to present the decoupling model, which can offer independent control for the refrigeration capacity and the degree of superheat for more efficient operation. As a result of the variations in the compressor frequency and the EEV opening, the dynamic models consider the transition state of the operations and the effects related to the variations on the chamber temperature and the superheat. Then, the presented control

system can be used for single input single output(SISO) system, where the controller may be readily designed. Next, the PI controller scheme with decoupling model is presented to control the thermal capacity and superheat independently for saving energy and progress of COP. The general PI controller without interfering loops inside has been successfully designed, and the experimental results show that the presented PI controller with the feedforward compensator is effective method of controlling the VSRS. Finally, the fuzzy control method is presented to control the capacity and superheat without troublesome dynamic model of the system. Some experimental result predicted that the proposed fuzzy controller is suitable for the capacity and superheat control of the VSRS. To improve transient response, the fuzzy control with feedforward compensator is proposed in this study.

1.2 Review of the previous studies

Willatzen et al. [16~29] presented a mathematical model describing the transient phenomena for two-phase flow heat exchangers. The refrigerant flow inside the coil of the heat exchange can be distinguished into two completely different types, two-phase flow and single-phase(liquid, vapor) flow. Based on the partial-differential equations representing mass and energy conservations, a set of ordinary-differential equations is formulated, taking into account the three zones in a heat exchanger. Two numerical models [30~37] were proposed to simulate the transient and steady behavior of a vapor compression refrigeration system. It is known that the condenser and the evaporator can be divided into a number of control volumes. Then, a system of time dependent partial differential equations can be obtained, considering the mass, energy and momentum balances for each control volume. Since the expansion valve and the compressor have very small inertia, the steady-state models can be employed for such components. The precise mathematical model is useful for the transient analysis of thermal plant in numerical simulations. Unfortunately, it is not directly applicable to

real control system design due to the involved complexity of precise model considering high order terms. For more efficient and systematic design of the controller, a dynamic model is to take into account the control parameters as well.

Outtagarts et al. [38] have presented that the superheat variations in the refrigerant mass flow rate can be ascertained using first-order model with delay. The evaporator gain, time constant, and delay are found to depend on two parameters; evaporating temperature and compressor speed, obtained from experiments. Aprea et al. [39] deduced a transfer function for a direct air-cooled evaporator, inserted in a vapor compression refrigeration plan by means of experimental analysis. The evaporator dynamic behavior is simulated by a first-order model with delay by taking into account the inlet air temperature (onto the evaporator) and the refrigerant mass flow rate. Choi et al. [40~42] developed first-order lumped-parameter empirical models based on experiments with various test conditions. Parameters in the models were assumed as the function of the indoor temperature, the compressor speed, and the percentage of the expansion valve opening. The empirical models were assumed as the first order model with time delay, and the parameters were determined by the method of regression analysis with a number of experiments.

Choi et al. [43~44] suggested a superheat control method with feedforward for variable speed heat pump system, in which the compressor frequency was determined by an empirical equation using regression analysis. In case of the control system based on the empirical model, it inevitably exhibits fairly large steady-state errors. Since the capacity controller considered the steady-state case only, the superheat controls have huge overshoot and undershoot. To overcome these problems, this research proposed a decoupling model to eliminate the interfering loops between the capacity and the superheat. Then, they designed PI controller with feedforward compensator to handle the thermal capacity and the superheat independently.

A fuzzy control algorithm was implemented by Han et al. [45~48] to

avoid the usage of the dynamic system model. The fuzzy control algorithm was developed to control the compressor speed of a multi-type air-conditioning system. Kim et al. [49] developed the fuzzy algorithm to control the superheat of the refrigeration system. In addition, Han et al. [50] proposed control system based on fuzzy control inference using multiple input variables. The control algorithms for the compressor and the electronic expansion valve of a multi-type air-conditioning system were developed by using fuzzy logics. The input variables of compressor frequency control were composed of outdoor temperature, the number of using heat exchanger, indoor temperature, and the variation of the indoor temperature. The input variables of superheat control were composed of indoor temperature and the variation of indoor temperature. This thesis wants to propose control system based on the fuzzy control inference using single input value. It offers simultaneous control of the capacity and superheat without troublesome dynamic model. Such method can provide better control performance for the refrigeration system in spite of its inherent strong nonlinear characteristics.

1.3 The contents and outline of this research

Fig. 1.1 shows the objective of this thesis and the thesis has there objectives. The first is to develop the decoupling model, which can offer independent control for the refrigeration capacity and the degree of superheat for more efficient operations. The second is to design PI controller with feedforward compensator using presented decoupling model. Finally, the fuzzy control algorithm with feedforward compensator is proposed to control the capacity and superheat without troublesome dynamic model.

Chapter 1 is an introduction, introduces the background and objective of this thesis, and reviews the previous research. It also gives the outline and summary of contributions.

Chapter 2 proposes decoupling model, which can offer independent control for the refrigeration capacity and the degree of superheat for more efficient operation. As a result of the variation in the compressor frequency

and the EEV opening, the dynamic models consider the transition state of VSRS operation conditions and the effect related to the variation on the chamber temperature and the superheat.

Chapter 3 deals with independent control method for the VSRS based on general PI control law and fuzzy control algorithm. The PI control with feedforward compensator is designed based on the presented decoupling model in the first part of this chapter. The decoupling control scheme with feedforward compensator does not contain any interfering loops inside; it is possible to design the PI controller symmetrically. The fuzzy controller proposed in second part of this chapter aimed at simultaneous control of the capacity and superheat without troublesome dynamic model of the system. The proposed controller enables maximum COP and energy saving at the same time even though the control reference or thermal load is varied.

Chapter 4 presents conclusions and summarizes the results of this thesis.

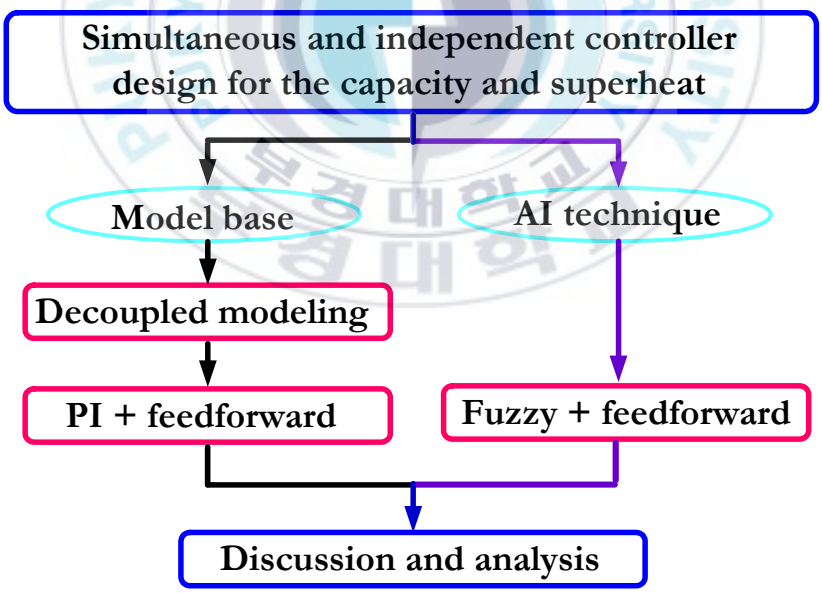

Fig. 1.1 Objective of this thesis

Chapter 2

Decoupled control modeling

In order to guarantee high efficiency and energy saving capability for the VSRS, a convenient mathematical model is crucial to design the control system. All the components in the refrigeration cycle are linked with pipes, demonstrating inherently nonlinear behaviors. Hence, it is unfeasible to exactly identify dynamic characteristics of practical refrigeration system. The precise mathematical model based on mass and energy conservative law has involved complexity and high-order term, it is not directly applicable to real control system design. On the other hand, in the proposed empirical model, the parameters were determined by an empirical equations using regression analysis. For more efficient and systematic design of the controller, a practical dynamic model must be presented. In this chapter, the dynamic model for the VSRS will be of interest.

2.1 Introduction of decoupling model

Fig. 2.1 shows a block diagram of refrigeration system with interfering loops featuring inside the dash dot and the dash two dot lines. The controlled variable is the quantity or condition that is measured and controlled. In this study, the controlled variables are the chamber temperature T_a and the degree of superheat SH. The superheat of evaporator is actually defined as the difference between the refrigerant vapor temperature and the saturation temperature at evaporator outlet. If there is no pressure drop or very small drop in the evaporator, the inlet temperature is almost equal to the saturation temperature at evaporator outlet. Then without loss of generality, the superheat can be defined as the temperature difference of refrigerant between outlet T_{eo} and inlet T_{ei} of the evaporator, i.e., $SH = T_{eo} - T_{ei}$. It is clear that the capacity and the

degree of superheat can not be manipulated separately due to the coupling characteristics of the refrigeration system.

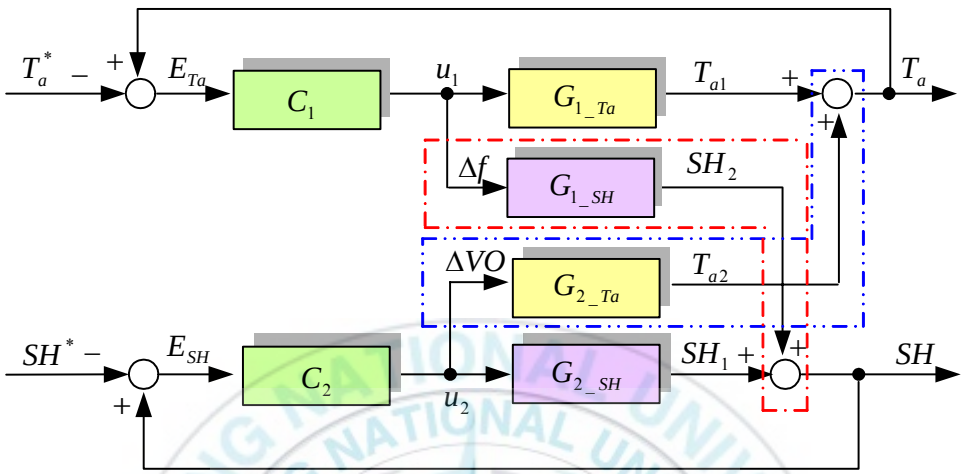

Fig. 2.1 Block diagram of VSRS control system with interfering loops

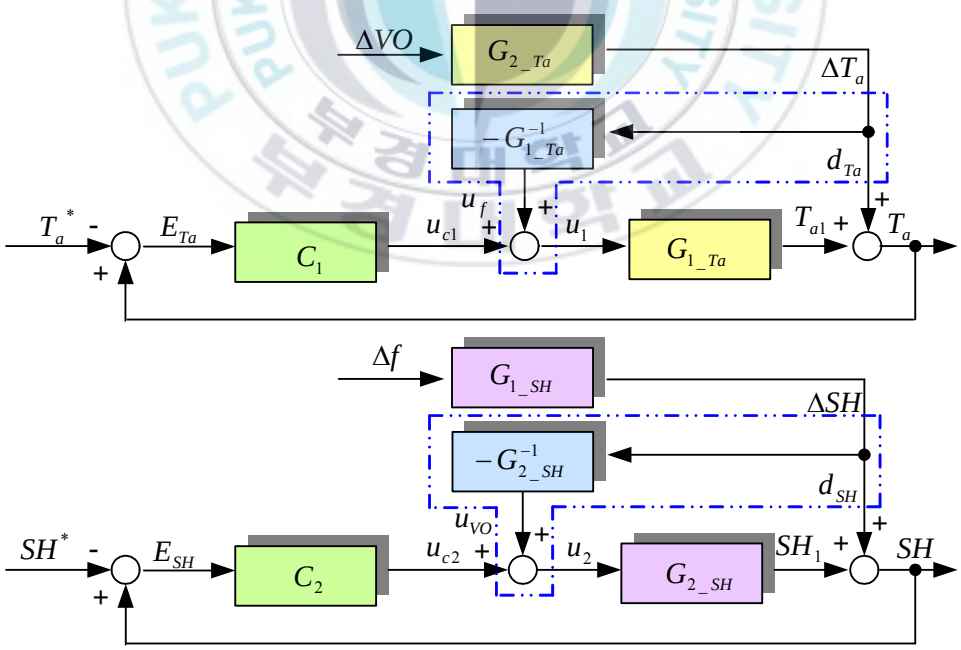

Fig. 2.2 Block diagram of decoupling control for VSRS

Hence, the transfer functions for T_a and SH with respect to their references are expressed as

$$\frac{T_a}{T_a^*} = \frac{-C_1G_{1\_Ta} + C_1C_2G_{1\_Ta}G_{2\_SH} - C_1C_2G_{1\_SH}G_{2\_Ta}}{1 - C_1G_{1\_Ta} - C_2G_{2\_SH} + C_1C_2G_{1\_Ta}G_{2\_SH} - C_1C_2G_{1\_SH}G_{2\_SH}} - \frac{C_{2\_SH}G_{2\_Ta}}{1 - C_1G_{1\_Ta} - C_2G_{2\_SH} + C_1C_2G_{1\_Ta}G_{2\_SH} - C_1C_2G_{1\_SH}G_{2\_Ta}} \frac{SH^*}{T_a^*} \tag{2-1}$$

$$\frac{SH}{SH^*} = \frac{1 - C_2G_{2\_SH} + C_1C_2G_{1\_Ta}G_{2\_SH} - C_1C_2G_{1\_SH}G_{2\_Ta}}{1 - C_1G_{1\_Ta} - C_2G_{2\_SH} + C_1C_2G_{1\_Ta}G_{2\_SH} - C_1C_2G_{1\_SH}G_{2\_SH}} - \frac{C_1G_3}{1 - C_1G_{1\_Ta} - C_2G_{2\_SH} + C_1C_2G_{1\_Ta}G_{2\_SH} - C_1C_2G_{1\_SH}G_{2\_Ta}} \frac{T_a^*}{SH^*} \tag{2-2}$$

where $C_i\,(i = 1\sim2)$ represents controller, and $G_i\,(i = 1\sim2)$ denotes transfer function. The individual reference levels are represented in T_a^* and SH^*. Furthermore, each closed-loop transfer function includes a set of controllers and transfer functions of the plants. As consequence, there exists the degree of complexity in design of controllers C_1 and C_2.

Next, Fig. 2.2 illustrates the schematic diagram for proposed decoupling control scheme, where it does not include interfering loops. Furthermore, the effect of parametric variations due to instance changes on opening angle ΔVO and compressor frequency Δf has been incorporated in the system's input side using feed-forward mode.

The simplified transfer functions with feedforward method can be given as

$$\frac{T_a}{T_a^*} = \frac{-C_1G_{1\_Ta}}{1 - C_1G_{1\_Ta}} \tag{2-3}$$

$$\frac{SH}{SH^*} = \frac{-C_2 G_{2\_SH}}{1 - C_2 G_{2\_SH}} \tag{2-4}$$

Based on the above transfer functions with reference to Fig. 2.2, the decoupled controllers can be systematically designed without interfering loops.

As established in references in [6~10], the variations of chamber temperature and superheat can be described by considering the first-order model with time delay. The proposed transfer function is

$$G_i = \frac{k_i}{1 + \tau_i s} e^{-L_i s} \tag{2-5}$$

where the model parameter DC gain k_i, the time constant τ_i, and the dead time L_i can be obtained using the experimental data for various possible operating conditions. It should be noted that the transfer function in Fig. 2.2 is given in the first-order model with delay, as represented by Eq. (2-5).

2.2 Decoupled control modeling by experiment

In this section, the extensive tests are performed to demonstrate the methodology on the VSRS model. A schematic diagram for the test setup is shown in Fig. 2.3, in company with photo. (see Photo. 2.1). The experimental system mainly consists of a basic refrigeration cycle, a control system, and a data acquisition system. Table 2.1 provides the detailed specifications for the test unit. The compressor in the refrigeration cycle is driven by the induction motor with a general V/f constant-type inverter. Stepper motor to drive EEV is operated through a step valve control interface. All temperatures are measured by using thermocouples (T-type) and temperature probes (Pt-100), saved in a data acquisition system in real time. Since the pressure drop in the evaporator is approximately

0.02~0.15bar, which can be practically negligible, the definition SH given before is valid the refrigeration type of R22. Furthermore, Fig. 2.4 shows the structure of the EEV and the functional relationship between input of the stepper motor and output of EEV is illustrated in Fig. 2.5.

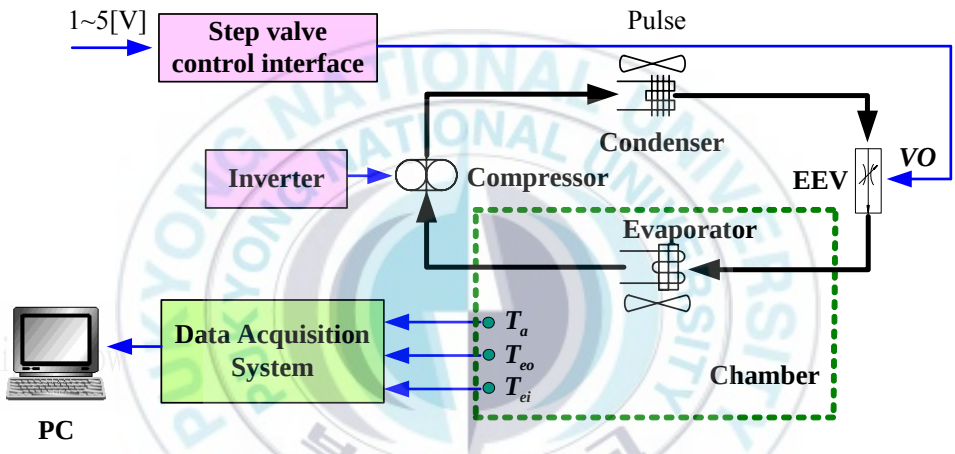

Fig. 2.3 Schematic diagram of the experimental system

Photo. 2.1 Experimental system

Table 2.1 Specifications of the test setup for modeling

Compressor	Vertical, Reciprocating, 220V, 60㎐, 1.5㎾
Condenser	Fin-tube type, capacity: 4㎾
Evaporator	Fin-tube type, capacity: 0.79㎾
Expansion Valve Device	Port size: Φ14㎜ Operating range: 0 ~ 506 pulse Rated voltage: DC 12V
Refrigerant	R22
Chamber	Size: 1200 x 700 x 1650[㎜]
Inverter	PWM type, 2HP
Step valve control interface	Input signal: DC 1~5V or 4~20㎃ Output: 0~400 step

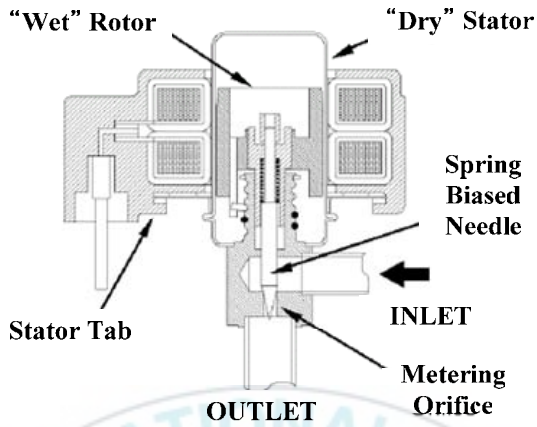

Fig. 2.4 The structure of the EEV

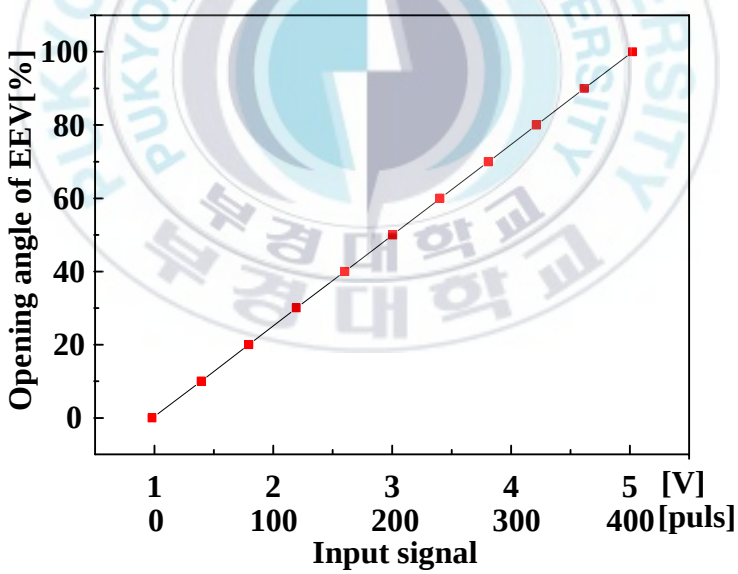

Fig. 2.5 The relationship between input signal and opening angle of EEV in stepper motor

In Fig. 2.2, the input variables of transfer functions are the variation of compressor frequency Δf and opening angle of EEV ΔVO; and the output variables are the variation of chamber temperature ΔT_a and the superheat ΔSH.

In this paper, the thermal loading and opening angle of EEV have been kept constant to observe the variations of ΔT_a and ΔSH due to the compressor speed changes. During the test, the compressor speed is varied in the range over 40~60㎐ with step size 10㎐. Based on experimental data, the transfer functions G_{1_Ta} and G_{1_SH} can be approximated to the following forms:

$$G_{1\_Ta} = \frac{\Delta T_a}{\Delta f} = \frac{-0.42}{680s+1} \tag{2-6}$$

$$G_{1\_SH} = \frac{\Delta SH}{\Delta f} = \frac{\Delta T_{eo}}{\Delta f} - \frac{\Delta T_{ei}}{\Delta f} = \frac{-0.47}{780s+1} - \frac{-0.15}{30s+1} e^{-25s} \tag{2-7}$$

where G_{1_Ta} and G_{1_SH} represent the variations of chamber temperature and superheat with regard to the compressor frequency, respectively.

Fig. 2.6 shows the comparison between experimental and simulation results for chamber temperature when the compressor frequency is varied from 40㎐ to 60㎐. The experimental data have been obtained under the following test conditions: the opening angle of EEV is set at 60% of the maximum value, and the thermal loading of 2.1㎾. In addition, the simulation results for chamber temperature are obtained using the transfer function G_{1_Ta} in Eq. (2-6) for the conditions identical to those maintained during experimentation. By comparison, the above transfer function fairly describes the dynamic behaviours of real system.

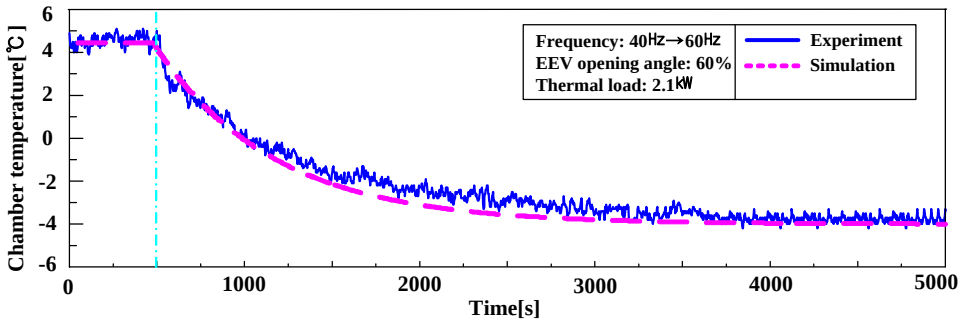

Fig. 2.6 Chamber temperature responses when the compressor frequency is varied

The temperature variations at inlet and outlet of evaporator are illustrated in Fig. 2.7. In addition, the experimental and simulation results for superheat response are shown in Fig. 2.8. The test conditions considered are the same as in the previous case. As noted, the experimental results of superheat do not offer the dynamic characteristics of the first-order system with dead time. Depending on the compressor frequency, the time constant for the evaporator temperature at outlet is observed considerably larger, compared to the inlet temperature, i.e., 780 seccond >> 30 second. Due to the different time constants of inlet and outlet, the rise in degree of superheat is observed for initial few minutes of operations. In a while it started on decreasing as the compressor frequency is increased. The variation tendency for evaporator inlet and outlet temperature is obtained to express the transfer function as first order system with dead time. In order to design the controller, the Eq. (2-7) is further simplified using Padé Approximation to

$$G_{1\_SH} \approx \frac{-131.1s^2 + 7.612s - 0.0256}{23400s^3 + 2682s^2 + 65.8s + 0.08} \tag{2-8}$$

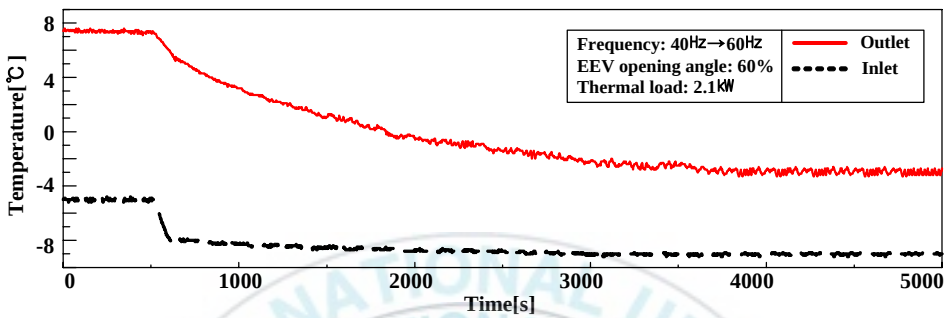

Fig. 2.7 Refrigerant temperature variations at inlet and outlet of an evaporator

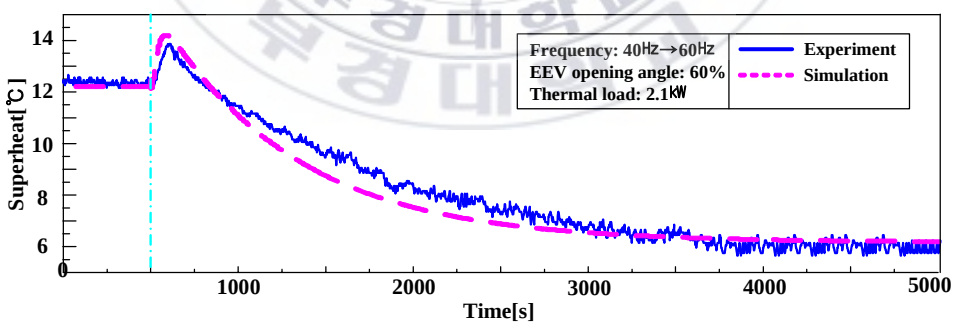

Fig. 2.8 Superheat responses when the compressor frequency is varied

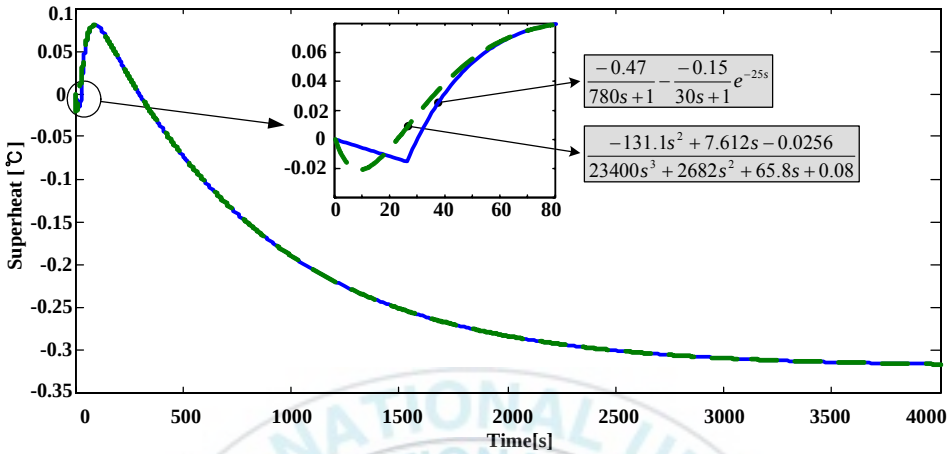

Fig. 2.9 Step responses of superheat with the compressor frequency

Fig. 2.9 shows the step responses for the models given in Eqs. (2-7) and (2-8), observing that the maximum error for both models occurs near 0.02℃. Note that the dashed line in Fig. 2.9 represents the simulation result of superheat response using G_{1_SH}. The experimental and simulation results show that the system model in Eq. (2-8) moderately represents the system performance.

Depending on the opening angle of EEV, the variations of ΔT_a and ΔSH has been obtained while the thermal load and compressor frequency are kept constant; the test opening angles of EEV are 5%, 10%, 15% and 20% of the maximum value. Using the experimental results, the transfer function G_{2_SH} can be deduced as

$$G_{2\_SH}=\frac{\Delta SH}{\Delta VO}=\frac{-0.38}{57s+1}e^{-16s} \tag{2-9}$$

Furthermore, the transfer function G_{2_SH} can be expressed using Padé

Approximation as

$$G_{2\_SH} \approx \frac{0.38s - 0.0475}{57s^2 + 8.125s + 0.125} \tag{2-10}$$

Fig. 2.10 shows the step responses for the models given in Eqs. (2-9) and (2-10), where the maximum discrepancy now occurs near 0.015℃. In Fig. 11, the solid line explains the experimental result of superheat response when the opening angle of EEV is abruptly changed from 70% to 55% of the maximum value at 200 second. In this test, the compressor frequency is set at 40㎐, and the thermal load is kept near 1.8㎾. The dashed line demonstrates the simulation result for the superheat response for G_{2_SH}. It can be observed from Fig. 2.11 that the simulation result is reasonably close to the experimental result. While maintaining the same test conditions in Fig. 2.11, Fig. 2.12 describes the chamber temperature response against variations of the opening angles of EEV, G_{2_Ta}. It shows that the variation of chamber temperature has been increased less than 1℃ The experimental result indicates that the variation of chamber temperature is very small, comparing to that of superheat for the given opening angle of EEV. Therefore, the transfer function G_{2_Ta} could be ignored for practical purposes.

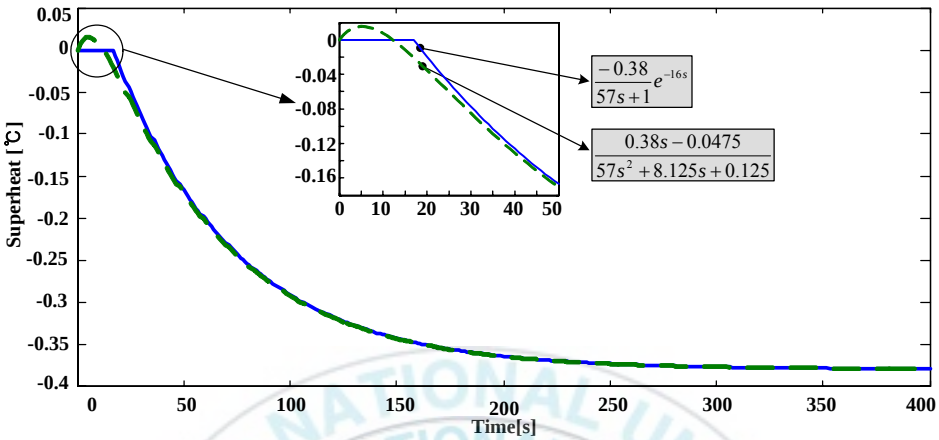

Fig. 2.10 Step responses of superheat with the opening angle of EEV

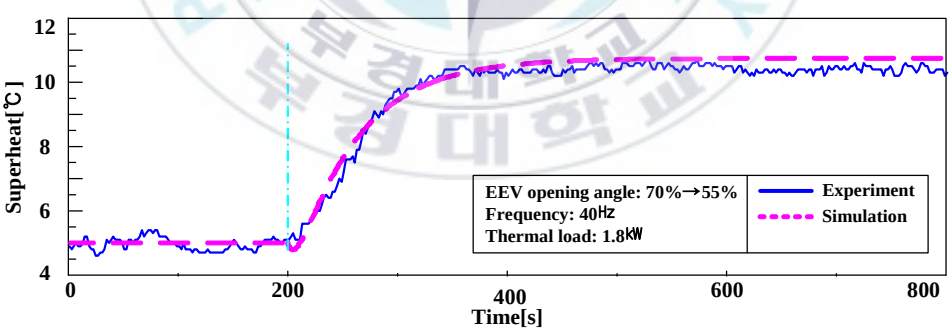

Fig. 2.11 Superheat responses when the opening angle of EEV is varied

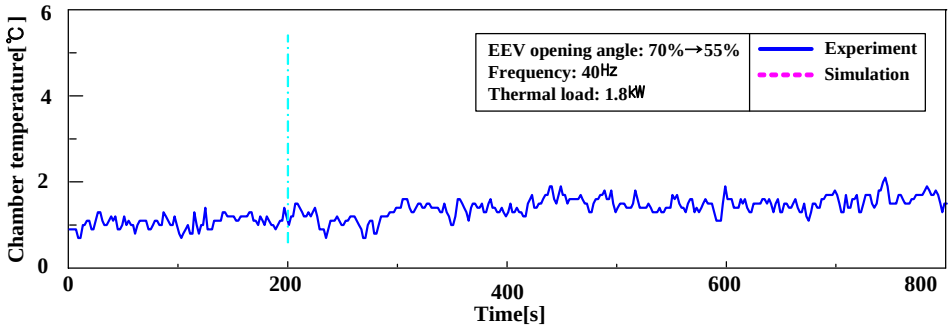

Fig. 2.12 Chamber temperature response when the opening angle of EEV is varied

2.3 Analysis of the sensitivity of the decoupling model

To estimate the exactitude of the empirical models, the sensitivity of the decoupling model has been analyzed with simulation method. It is given ±10% errors to the DC gain, time constant, and time delay of the models. The proposed models are compared with the models with errors. Fig. 2.13 shows the analysis of parameters sensitivity of the transfer function G_{1_Ta}. Fig. 2.13(a) and Fig. 2.13(b) present the simulation results when model has ±10% DC gain errors and time constant errors respectively. They represent that the DC gain error only affects the steady state and the time constant error has an effect on the transient state. Fig. 2.14 describes the analysis of parameters sensitivity of the transfer function G_{1_SH}. Fig. 2.14(a), Fig. 2.14(b), and Fig. 2.14(c) show the simulation results when model has ±10% DC gain errors, time constant errors, and time delay errors respectively. The DC gain error has an influence upon the steady state, the error of time constant and time delay affect transient state, but the time delay error has little effect on the model. Fig. 2.15 presents the analysis of parameters

sensitivity of the transfer function G_{1_SH}. Fig. 2.15(a), Fig. 2.15(b), and Fig. 2.15(c) show the simulation results when model has ±10% DC gain errors, time constant errors, and time delay errors respectively. The simulation result have the same conclusion with transfer function of G_{1_SH}.

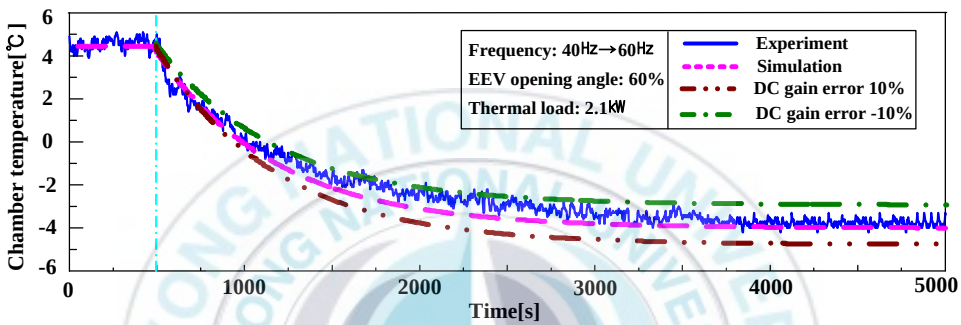

(a)

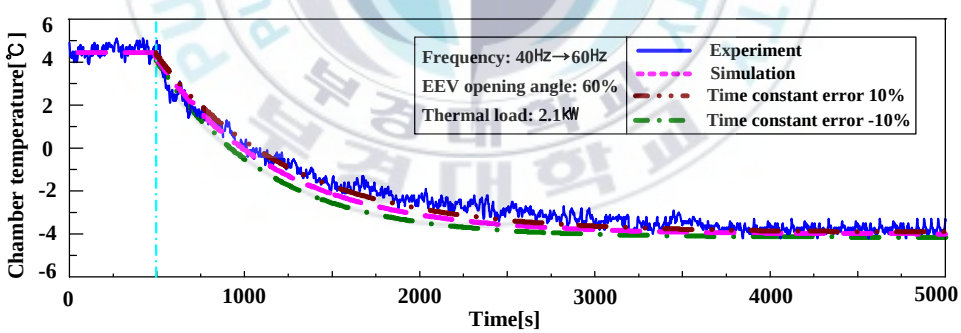

(b)

Fig. 2.13 Analysis of parameter sensitivity of G_{1_Ta}

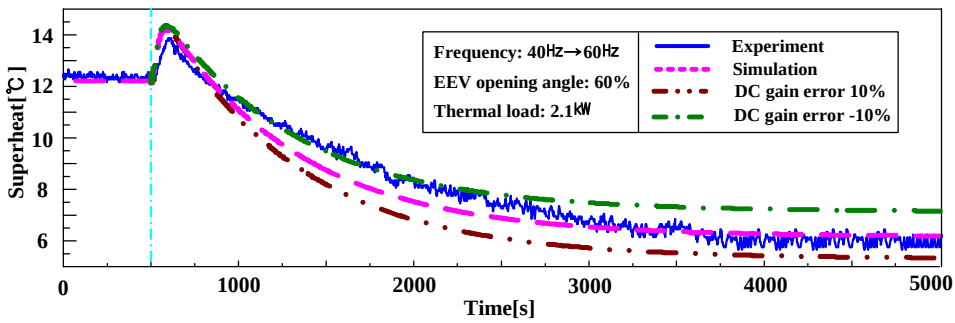

(a)

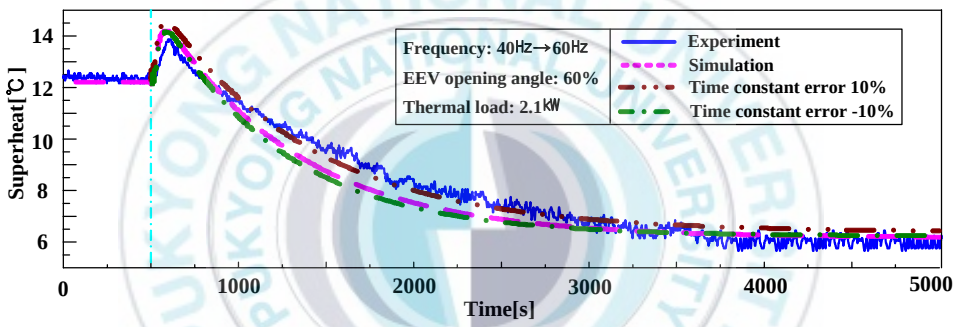

(b)

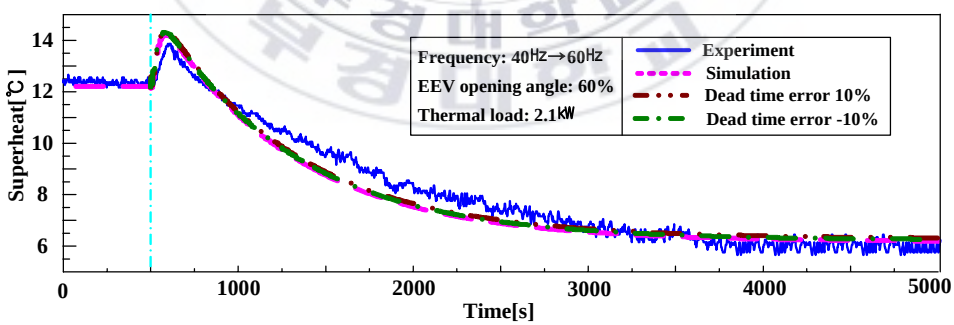

(c)

Fig. 2.14 Analysis of parameter sensitivity of G_{1_SH}

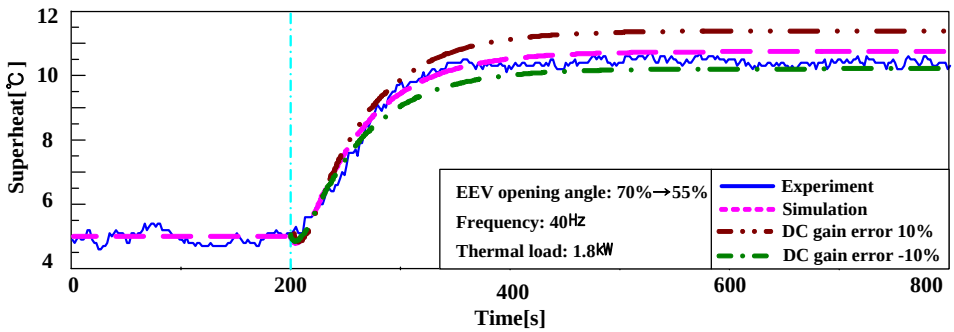

(a)

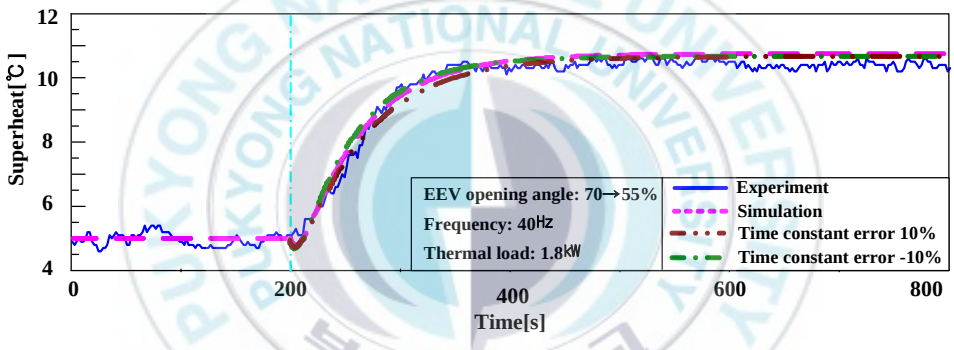

(b)

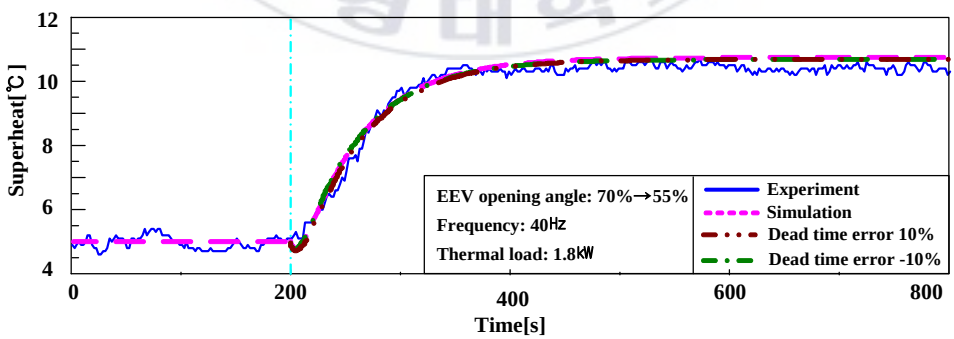

(c)

Fig. 2.15 Analysis of parameter sensitivity of G_{2_SH}

2.4 Summation of decoupling model

This chapter deals with the empirical dynamic models for decoupling control of the VSRS. The decoupling models have been presented to control the capacity and superheat independently and they are obtained from several experiments under various operating conditions. Key conclusions can be made as follows:

(1) The empirical models to control capacity and superheat are expressed as a simple first-order system, guaranteeing the maximum overall error of less than ±1℃.

(2) The test results strongly indicate that the proposed models are conveniently employed to formulate a robust control algorithm for regulating the VSRS.

(3) It has been confirmed by both theoretically and experimentally that the decoupling models is definitely practical for controlling the VSRS under variable operating conditions.

Chapter 3

Design of decoupling controller

Control means measuring the value of the controller variable of the system and applying the manipulated variable to the system to correct or limit deviation of the measured value from a desired value. In the VSRS, measuring the actual chamber temperature or superheat and comparing it with the reference temperature or superheat, the error signals are fed to the controller so as to reduce the error and bring the output of the system to the desired values.

Some of conventional controls are PID control, optimal control, adaptive control, nonlinear methods, etc. The convention controls are focused on modeling and use of this model to construct a controller. Over 90% of the controllers in operation today are PID controllers. This approach is often viewed as simple, reliable, and easy to understand.

Basically, it is the difficult task of modeling for control systems development. Even if a relatively accurate model of dynamic system can be developed, it is often too complex to use in controller development. A model is not needed to develop a fuzzy controller, and this is the main advantage of the approach.

Hence, two kinds of control method, PID control based on model and Fuzzy control without model, are presented in this research to control the chamber temperature and superheat of VSRS.

3.1 Design of PI controller

PID(proportional-integral-derivative) control is certainly the most widely used control strategy today. It is estimated that over 90% of control loops employ PID control, quite often with the derivative gain set to zero(PI control). Over the last half-century, a great deal of academic and industrial

effort has focused on improving PID control, primarily in the areas of tuning rules, identification schemes, and adaptation techniques.

The proportional tem responds immediately to the current error, yet typically can not achieve the desired set point accuracy without an unacceptably large gain. The integral term yields zero steady-state error in tracking a constant set point, a result commonly explained in terms of the internal model principle and demonstrated using the final value theorem. Integral control also enables the complete rejection of constant disturbances. Derivative action combats the problem by sassing a portion of the control on a prediction of future error. Unfortunately, the derivative term amplifies higher frequency sensor noise; thus, a filtering of the differentiated signal is typically employed, introducing an additional tuning parameter.

PI controller is particularly common, since derivative action is very sensitive to measurement noise, and the absence of an integral value may prevent the system from reaching its target value due to the control action.

3.1.1 Design of PI controller and simulation

Fig. 2.2 depicts the block diagram of the decoupling control scheme with feedforward compensator. The controlled variables are chamber temperature T_a and the superheat SH, in which the superheat is the temperature difference of refrigerant between outlet and inlet of the evaporator. The block diagram does not contain any interfering loop inside. Furthermore, each influence of operating variations such as opening angle ΔVO and compressor frequency Δf is considered on the corresponding input side of the diagram with feedforward manner.

The PI controller based on the decoupling model is designed to manipulate the capacity and superheat of refrigeration system independently. The control action $u(t)$ is described by

$$u(t) = K_p e(t) + K_i \int_0^t e(t)dt = K_p[e(t) + \frac{1}{T_i}\int_0^t e(t)dt] \tag{3-1}$$

where K_p is the proportional gain, K_i is the integral gain, and T_i is integral time. The proportional value determines the reaction to the current error; the integral determines the reaction based on the sum of the recent errors.

The gains are tuned by the Ziegler-Nichols rules[51]. Ziegler-Nichols proposed rules for determining values of the proportional gain K_p, integral time T_i, and derivative time T_d. There are two methods called Ziegler-Nichols tuning rules: the first method(based on step response of plant) and the second method(based on critical gain and critical period). In the first method , we obtain experimentally the response of the plant to a unit-step input. If the plant involves neither integrator nor dominant complex-conjugate poles, then such a unit-step response curve may look S-shaped curve. This method applies if the response to a step input exhibits an S-shaped curve. The S-shaped curve may be characterized by two constants, delay time and time constant. With the two constants, Ziegler-Nichols suggested to set the values K_p, T_i, and T_d according to the formula. In the second method, using the proportional control action only, increase K_p from 0 to a critical value K_{cr} at which the output first exhibits sustained oscillations. Thus, the critical gain K_{cr} and the corresponding period P_{cr} are experimentally determined. Ziegler-Nichols suggested to set the values of the parameters K_p, T_i, and T_d according to the formula.

In this study, the experimental models are given in the previous research in Chapter 2.

It seems obvious that the controllers for the chamber temperature and superheat are designed separately. Simulation studies can be used in early design stages to determine values for parameters. In the simulations, the ranges of Δf and ΔVO have been set as $30\sim60$Hz and $10\sim100\%$, respectively. It is assumed that the control periods for capacity and the superheat are respectively 30 and 15 seconds. The T_a and SH are both control variables whose specific values are assigned depending upon system objectives and characteristics. As stated in the paper, the SH represents the

superheat describing the temperature difference between the outlet and the inlet of the evaporator. From the maximum COP obtained by the experiment, it is set to 6℃.

Fig. 3.1 shows the PI control response of chamber temperature when the control reference is rapidly varied from 4℃ to 0℃ at 200 second with keeping the opening angle of EEV constant (at 80% of its maximum). For the capacity control, the gains are tuned by the Ziegler-Nichols rules based the critical (oscillation) frequency response method (second method). The gain K_{cr} and the period P_{cr} obtained are 1600 and 900sec, respectively. Based on K_{cr} and P_{cr}, the gains K_{p1} and K_{i1} have been calculated as 720 and 0.95, respectively. Through minor adjustments, the gains K_{p1} and K_{i1} have been finally determined as 800 and 0.2, respectively. It is noted that the superheat does not maintain the initial value, and it is changed with the variation of compressor frequency. Thus, it is required to handle the superheat along with the variation of compressor frequency.

Fig. 3.2 shows the superheat responses of the coupled control. The gains are tuned by the Ziegler-Nichols rules based on the step (or indicial)-response method (first method). The proportional gain K_{p2} is 20 and integral gain K_{i2} is 0.4 for the coupled control. As illustrated in Fig. 3.2(a), the percent overshoot is 50%, the undershoot is 2℃, and the settling time is 550 seconds with the coupled control method. Fig. 3.2(b) illustrates the control reference of compressor frequency.

The control period has been determined by considering the scan time constraint in PLC (programmable logic controller) as well as the time constant for the plant along with Shanon's sampling frequency[52].

For the capacity control, since the critical period is 900sec, the control period should be less than 450sec by the Shanon's sampling frequency and simultaneously greater than PLC scan time. Consequently, it is determined as 30sec. For the superheat control, the control period should be below the time constant of 77sec and simultaneously above PLC scan time(500ms), thus it is chosen as 15sec.

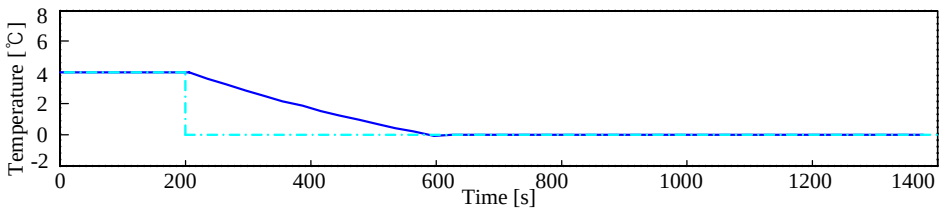

(a) The response of chamber temperature

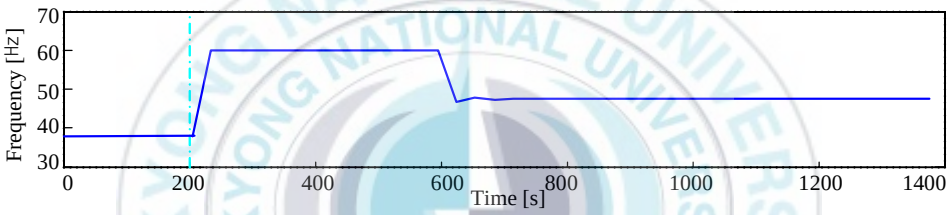

(b) The compressor frequency

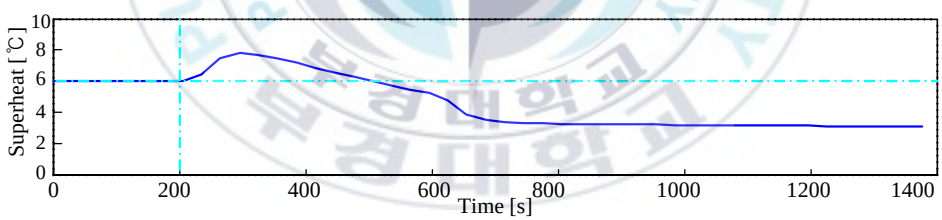

(c) The superheat response without control

Fig. 3.1 The simulation control response when the chamber temperature reference is varied.

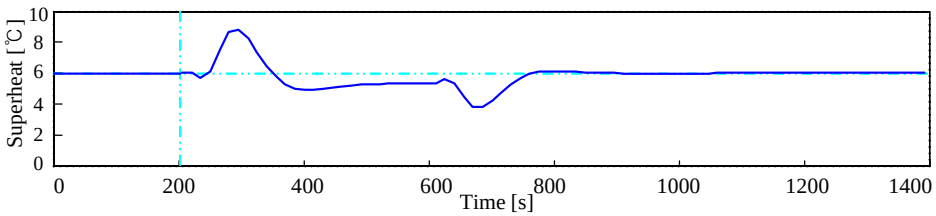

(a) The response of superheat to follow T_a reference

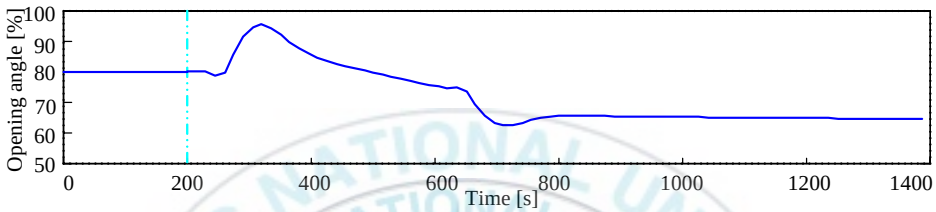

(b) The opening angle of EEV to follow T_a reference

Fig. 3.2 The simulation control response of coupled control

3.1.2 Experimental result of PI control and discussion

The schematic diagram of experimental system is illustrated in Fig. 3.3, in which the complete system includes the components of basic refrigeration cycle and control system. Table 2.1 and Table 3.1 summarize the main specifications of the experimental system. The key components of control system include an inverter, a step valve control interface, and a PLC (programmable logic controller) unit.

The compressor in the basic refrigeration cycle is driven by the induction motor with a general V/f constant type inverter. The step motor to drive EEV is operated by a valve control interface. The input signals of the inverter and the step valve control interface are received from a D/A unit of the PLC. The general PI control is implemented by a PID unit of the PLC, where all temperatures are measured by thermocouples (T-type). Then the

temperature information is transmitted to the thermocouple unit of the PLC with real time for operating input variables. Moreover, the thermal load of the chamber can be added by an electrical heater, and its magnitude is varied by the input voltage of the heater. Since the pressure drop in the evaporator is approximately 0.02~0.15 bar, which can be practically negligible, the definition of SH given before is valid the refrigerant type of R22.

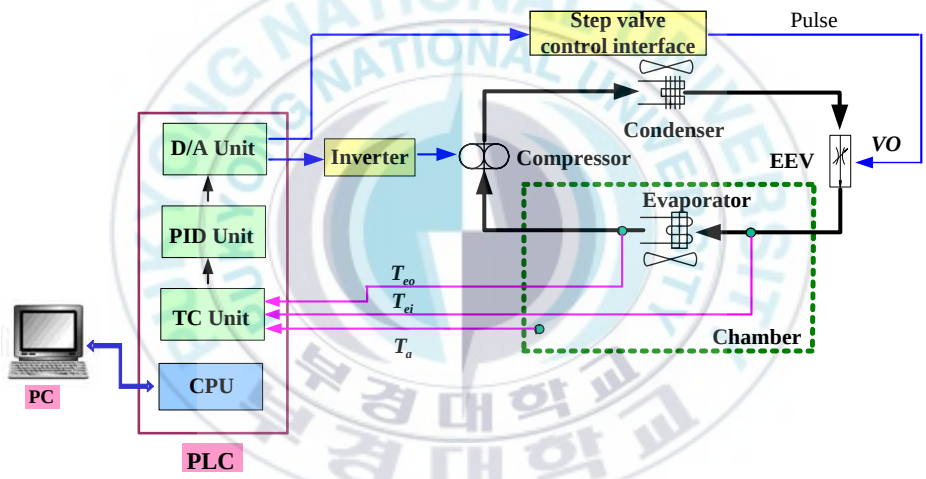

Fig. 3.3 Schematic diagram of the experimental system

Table 3.1 Specifications of the control unit of test

Inverter	Type	PWM
	HP	2
Step valve control interface	Input voltage	DC 12V
	Input signal	DC 1~5V or 4~20㎃
	Output	0~400 step
PLC	CPU	GM2
	PID unit	32 loop
	TC unit	16 Ch.
	D/A unit	16 Ch.

In this study, the fans have been maintained at constant speeds (rpm) for the condenser and the evaporator. As the compressor speed varies, the evaporating and condensing temperatures are definitely varying. More precisely, as the compressor speed increases, the evaporating temperature (pressure) is decreasing, and the condensing temperature moves up, and vice versa.

The compressor performance is determined by the amount of the actual required power into compressor, defined as follows:

$$\text{Actual compressor work} = \frac{\text{ideal compressor work[kW]}}{\text{compression efficiency} \times \text{mechanical efficiency}} \quad (3\text{-}2)$$

The mechanical efficiency is related to surface roughness, lubrication, and maintenance of the compressor, and it is approximately 0.8~0.95. Thus the required compressor power mainly depends on the compression efficiency. The higher compression efficiency it has, the better performance it has (i.e., the less the actual required power it has).

On the other hand, the compressor work mainly depends upon its

volumetric efficiency. Then the volumetric efficiency depends upon the speed of compressor: the higher speed it has, the less volumetric efficiency it has. However, if the compressor has very low speed, the volumetric efficiency also deteriorates due to the increase of the leaking vapor refrigerant. If the volumetric efficiency decreases, then the compressor work increases. Thus, to reduce the compressor work, we should obtain high volumetric efficiency at the optimal speed accompanying with high compressor performance.

The relationship between compressor power and thermal load are described in Fig. 3.4, where the superheat is maintained at 4~8℃. It can be seen that approximately 1㎾ electric power is required at operating conditions of compressor frequency 60㎐, thermal load 2.3㎾, and the chamber temperature 1℃. Supposing that the ambient thermal load is only varied to 2.06㎾ from initial condition 2.3㎾, the compressor frequency will be decreased to 40㎐. The power required for this condition is only 0.7 ㎾. Consequently, the variable speed compressor can save energy up to 30% as the thermal load changes actively, comparing with the case in the constant speed compressor.

In general, the COP is defined as follows:

$$\mathrm{COP} = \frac{\mathrm{cooling\,capacity[kW]}}{\mathrm{work\,input[kW]}} \tag{3-3}$$

In this formulation, the work input only takes into account the work consumed by the compressor. The energy consumed in other fans (such as in the evaporator and condenser) is not included in this equation. The relationship between COP and superheat is shown in Fig. 3.5(a). In the experimental tests, the chamber temperature is kept at 1℃, and the compressor is operated at the frequencies of 40㎐, 50㎐, and 60㎐. There exists a difference in COP due to operating frequency while the superheat is kept the same. However, the COP has approximately the same value when superheat is at 0~8℃. Also, it is found that the COP is reduced according to

the increase of superheat over 8℃ at every compressor speed. Fig. 3.5(b) shows the relationship between COP and superheat according to change of chamber temperature. From this figure, it can be seen that the COP has also different value according to change of chamber temperature even though the superheat is kept the same. However, there exists very similar pattern in COP within superheat range 0~8℃, and it is also decreased gradually beyond 8℃ at the corresponding compressor speed.

An optimized system would lead at the highest evaporation pressure as possible as to reduce compressor work. However, it doesn't offer the best COP under the highest evaporation pressure. If the evaporating pressure is too high, the degree of superheat will be reduced and the refrigerant can not evaporate enough. Then liquid refrigerant can flow out of the evaporator with danger of liquid slugging to the compressor. Hence, it is important to control the expansion valve to obtain a best superheat.

To maintain high COP, the superheat must be kept as a certain constant temperature, regardless of the operating conditions such as compressor speed, chamber temperature, etc.

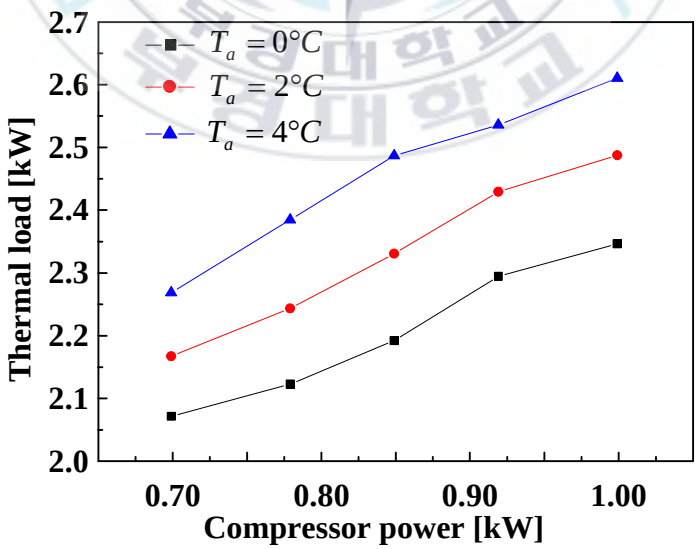

Fig. 3.4 Relationship between compressor power and thermal load

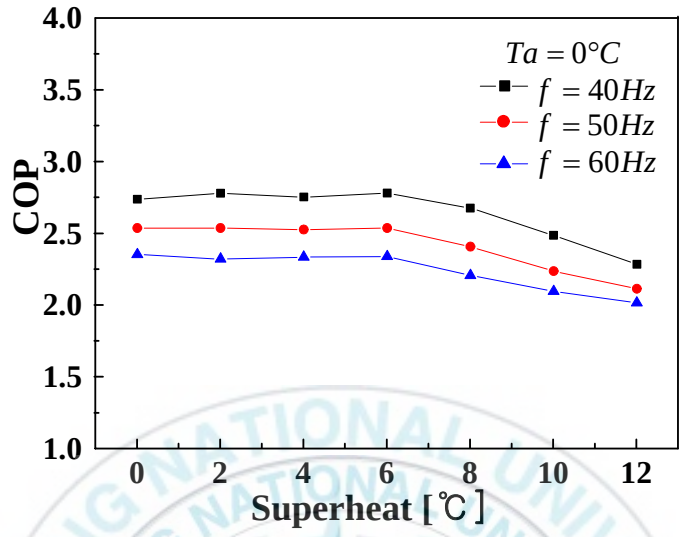

(a)

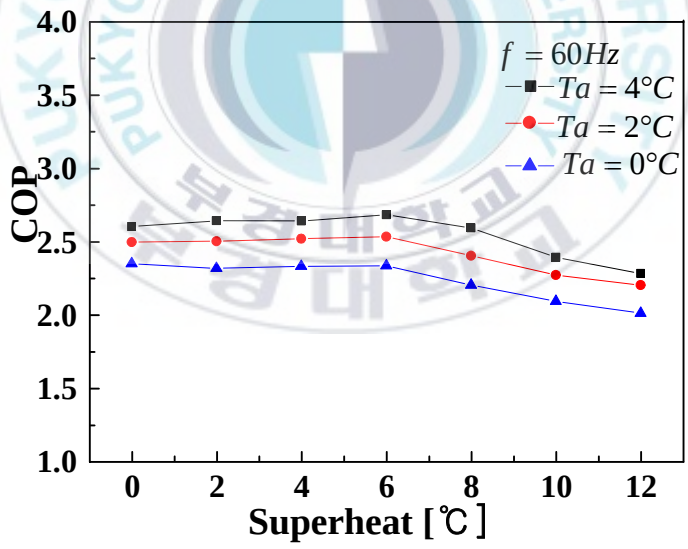

(b)

Fig. 3.5 Relationship between COP and superheat

In the experimental tests, the ranges of Δf and ΔVO are set to 30~60Hz and 10~100%, respectively. In addition, the control periods has taken 30 seconds for capacity and 15 seconds for the superheat. To describe phenomena simply, the Padé approximation and Taylor series expansions have been employed in this study.

Fig. 3.6 describes the PI control response of chamber temperature and superheat when the chamber reference temperature is abruptly varied from 4℃ to 0℃ at 200 second. The thermal load is 1.45㎾ and the superheat reference is 6℃. Fig. 3.6(a) shows the PI control response of chamber temperature when the reference is changed. It took about 450 seconds to reach close to a set point value from change of reference. Fig. 3.6(b) shows the response of compressor frequency to follow the reference of chamber temperature. It can be seen that the set point frequency of the compressor for controlling the capacity is extremely stable. Fig. 3.6(c) presents the PI control response of superheat according to the change of chamber temperature. The superheat must be controlled as a constant value even though the compressor speed and chamber temperature are varied. As depicted in this figure, the percent overshoot of the superheat observed is about 33%, and the maximum undershoot of superheat is about 30%. Fig. 3.6(d) shows that the set point value of EEV opening angle is changed stably to maintain the superheat at 6℃. Since the percent overshoot is fairly big, it is not acceptable for control performance. Thus, the PI controller with feedforward compensator has been proposed to improve the control performance.

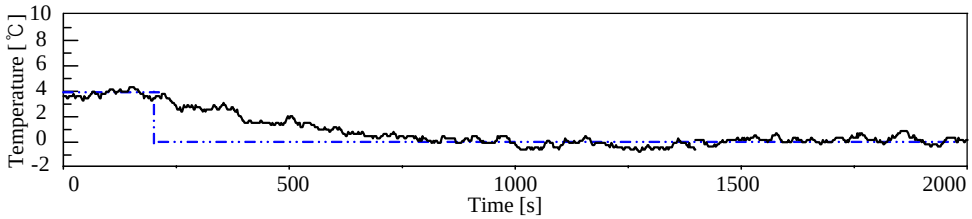

(a) The response of chamber temperature

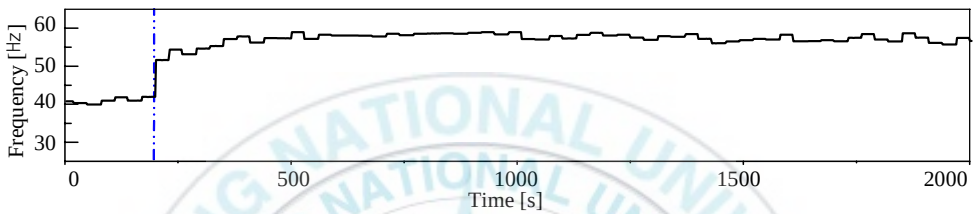

(b) The compressor frequency

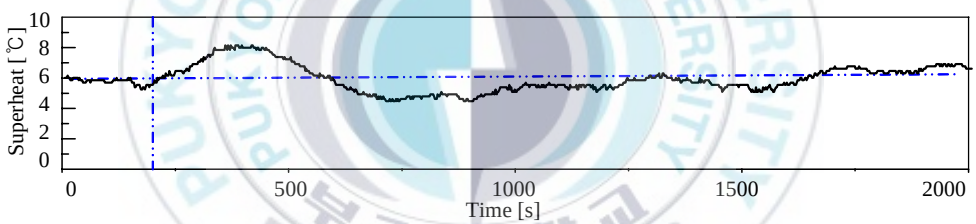

(c) The response of superheat

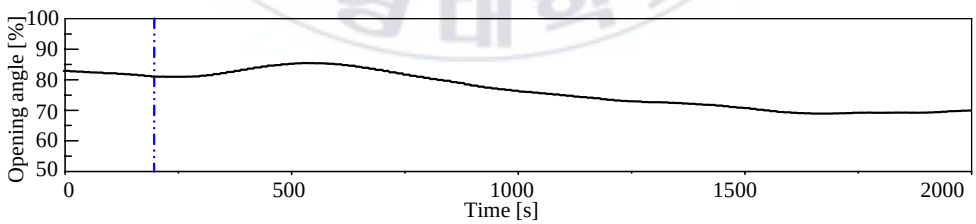

(d) The opening angle of EEV

Fig. 3.6 The responses of chamber temperature and superheat by PI control according to the change of chamber temperature reference ($T_a^* = 4^\circ C \rightarrow 0^\circ C$, $SH^* = 6^\circ C$, $Q = 1.45$ ㎾).

3.1.3 Design of PI controller with feedforward compensator and simulation

Generally speaking, it is desirable to manage the capacity and superheat simultaneously in the VSRS. However, simultaneous controller based on the conventional coupling model does not guarantee reasonable time-domain performances, such as overshoot/undershoot and settling time, due to the interference of the variations of compressor speed. In this paper, the PI control with feedforward compensator has been proposed to deal with these problems. In addition, it can eliminate the influence of the interfering loops on the capacity and superheat quantities.

In the refrigeration system, the disturbance $d(s)$ has also effect on superheat and chamber temperature caused by the variations of the compressor speed Δf and the opening angle ΔVO of EEV. Each disturbance input can be expressed as follows:

$$d_{SH}(s) = G_{1\_SH}\Delta f \tag{3-4}$$

$$d_{Ta}(s) = G_{2\_Ta}\Delta VO \tag{3-5}$$

To cancel the effect of this disturbance on the control system, the corresponding compensators are given as follows:

$$u_f(t) = -\pounds^{-1}[\frac{1}{G_{2\_SH}(s)}d_{SH}(s)] \tag{3-6}$$

$$u_{VO}(t) = -\pounds^{-1}[\frac{1}{G_{1\_Ta}(s)}d_{Ta}(s)] \tag{3-7}$$

where u_f and u_{VO} are compensating quantities of Δf and ΔVO,

respectively. Then, the effect of interference due to the variations of compressor speed and opening angle can be removed on the superheat and the chamber temperature.

The transfer function associated with T_a and SH with feedforward methods can be simply expressed as

$$\frac{T_a}{T_a^*} = \frac{-C_1 G_{1\_Ta}}{1 - C_1 G_{1\_Ta}} \tag{3-8}$$

$$\frac{SH}{SH^*} = \frac{-C_2 G_{2\_SH}}{1 - C_2 G_{2\_SH}} \tag{3-9}$$

Fig. 3.7 describes the responses of chamber temperature and superheat by PI controller with feedforward compensator when the control reference is rapidly varied from 4℃ to 0℃ at 200. Fig 3.7(a) shows the response of chamber temperature and Fig. 3.7(b) shows the response of compressor frequency. In this simulation the proportional gain K_{p1} is 800 and integral gain K_{i1} is 0.2. Finally, the superheat responses of the decoupling and coupled control schemes are described for comparisons. The gain tuning in superheat control is based on the indicial response for the plant. The time constant and time delay obtained are 77sec and 6.5sec, respectively. Then, K_{p2} and K_{i2} have been calculated as 10 and 0.46, respectively. Finally, the gains K_{p2} and K_{i2} have been chosen as 12 and 0.25, respectively. As illustrated in Fig. 3.7(c), the percent overshoot is 50%, the undershoot is 2℃, and the settling time is 550 seconds with the coupled control method. On the contrary, the percent overshoot is 0, the undershoot is 2℃, and the settling time is 550 seconds with decoupling controller. Fig. 3.7(d) illustrates the control reference of compressor frequency, in which the response of decoupling control is faster than coupled control case due to the feedforward compensator.

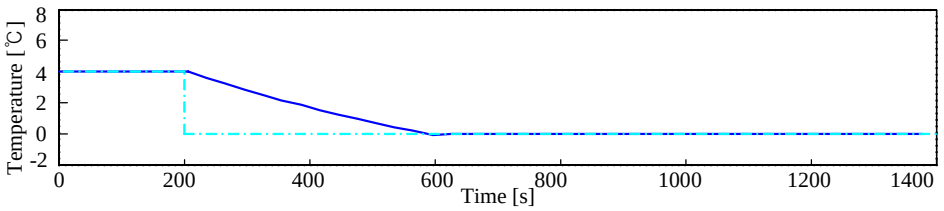

(a) The response of chamber temperature

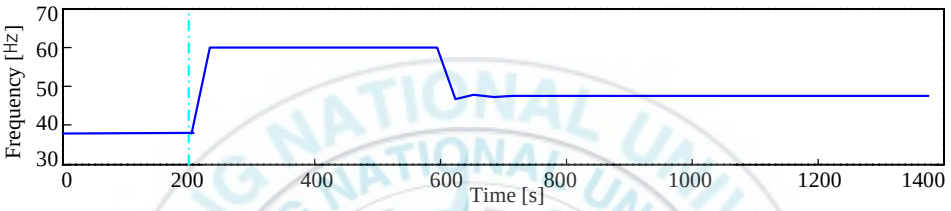

(b) The compressor frequency

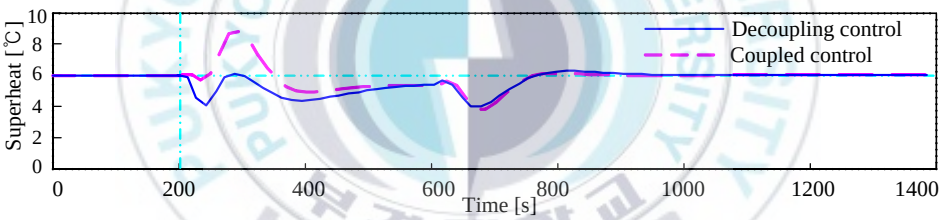

(c) The superheat response

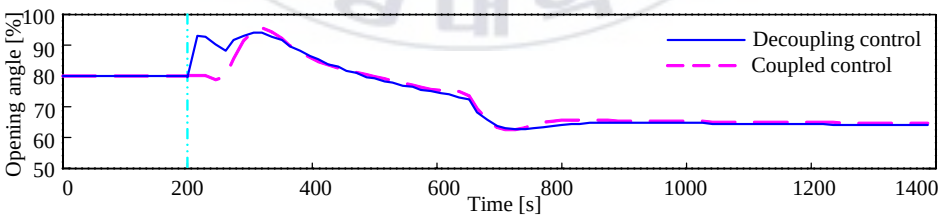

(d) The opening angle of EEV

Fig. 3.7 The simulation control response with decoupling control when the chamber temperature reference is varied.

In addition, the objectives of set point tracking and disturbance rejection are to minimize the error. For the fixed input(that is, disturbances and/or set point), two of the most popular performance measures are the integral absolute error(IAE) and the integral square error(ISE)[53]. The ISE is adopted in this research. The performance index is evaluated for a quantitative measure of the attained tracking performance as follows:

$$I_{e,T_a} = \int_{t_0}^{t_f} (T_a - T_a^*)^2 dt = 1.61 \times 10^6 \quad \text{(coupling or decoupling control)} \quad (3\text{-}10)$$

$$I_{e,SH} = \int_{t_0}^{t_f} (SH - SH^*)^2 dt = 5.98 \times 10^5 \quad \text{(coupling control)} \quad (3\text{-}11)$$

$$I_{e,SH} = \int_{t_0}^{t_f} (SH - SH^*)^2 dt = 5.38 \times 10^5 \quad \text{(decoupling control)} \quad (3\text{-}12)$$

Here, the start time t_0 and finish time t_f of integral are 200 sec and 800 sec, respectively(see Fig. 3.7). Since the effect of opening angle variation in EEV has been neglected on the chamber temperature, there exists no performance difference on the chamber temperature between coupling and decoupling controls. However, the compressor speed has definitely an effect on the superheat. The decoupling approach with feedforward compensation provides better control performance than coupling approach. Referring to the index $I_{e,SH}$, it is known that there exists 10% performance improvement in decoupling control.

3.1.4 Experimental result of PI control with feedforward compensator and discussion

Fig. 3.8 describes the responses of chamber temperature and superheat using the PI control with feedforward compensator while the chamber reference temperature is maintaining the same test conditions as previous experiment. Fig. 3.8(a) shows the PI control response of chamber temperature when the reference is changed. It took about 400 seconds to reach close to a set point value from change of reference. Fig. 3.8(b) shows the response of compressor frequency to follow the reference of chamber temperature. It can be seen that the set point frequency of the compressor for controlling the capacity is extremely stable. Fig. 3.8(c) presents the PI control response of superheat according to the change of chamber temperature. The superheat must be controlled as a constant value even though the compressor speed and chamber temperature are varied. As depicted in this figure, the percent overshoot of the superheat observed is about 15%, but the maximum overshoot is below 7℃. The maximum undershoot of superheat is above 5℃, which is acceptable value in the refrigeration system. Fig. 3.8(d) shows that the set point value of EEV opening angle is changed stably to maintain the superheat at 6℃. These experimental results are well consistent with the simulation results reported previously.

Fig. 3.9 illustrates responses of chamber temperature and superheat for PI control with feedforward compensator when thermal load is varied from 1.44㎾ to 1.57㎾, where the chamber temperature reference is set at 0℃ and the superheat reference is 6℃. From Fig. 3.9(a), it can be seen that the chamber temperature is maintained at 0℃ even if the thermal load is varied. Fig. 3.9(b) shows that the compressor frequency has been increased to control the chamber temperature as 0℃ caused by the increase of thermal load. Fig. 3.9(c) gives the PI control response of superheat depending upon the change of thermal load, where the superheat has been controlled as a constant value 6℃ to obtain high COP. Fig. 3.9(d) shows the opening angle

of EEV under the given thermal load. As a result, it is evident that the PI control system guarantees excellent performance for the capacity and superheat under various thermal loads.

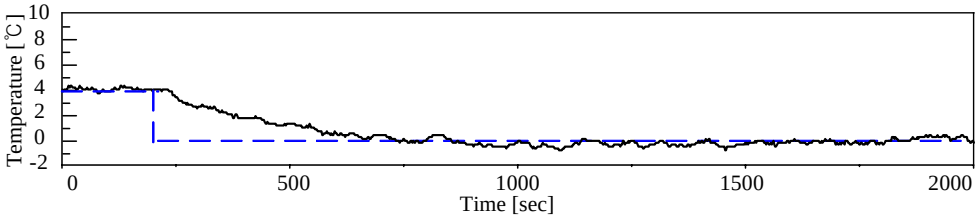

(a) The response of chamber temperature

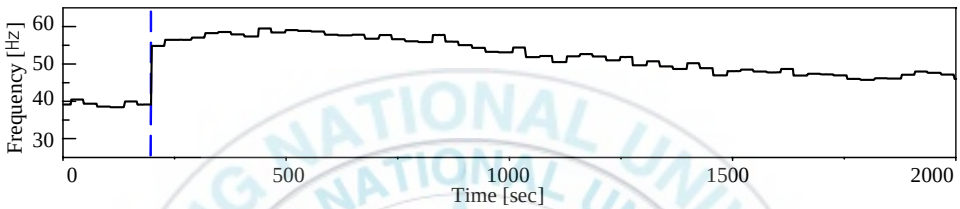

(b) The compressor frequency

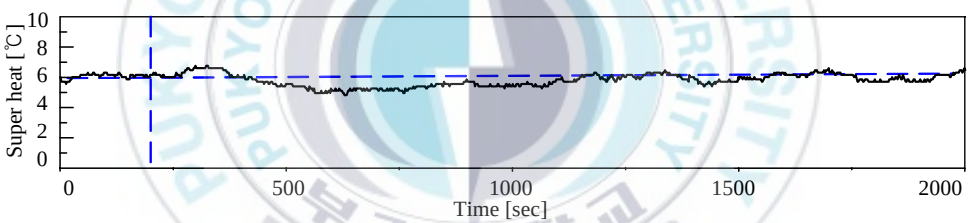

(c) The response of superheat

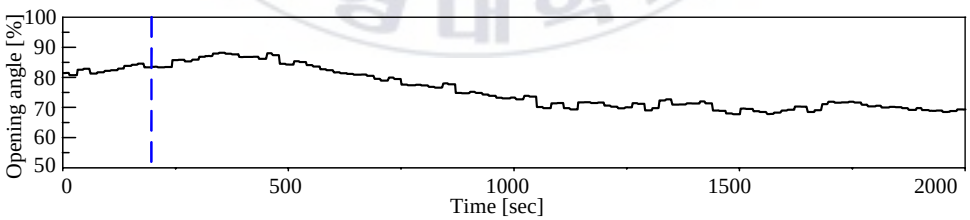

(d) The opening angle of EEV

Fig. 3.8 The responses of chamber temperature and superheat by PI control with feedforward compensator according to the change of chamber temperature reference($T_a^* = 4^\circ C \rightarrow 0^\circ C$, $SH^* = 6^\circ C$, $Q = 1.45$ ㎾).

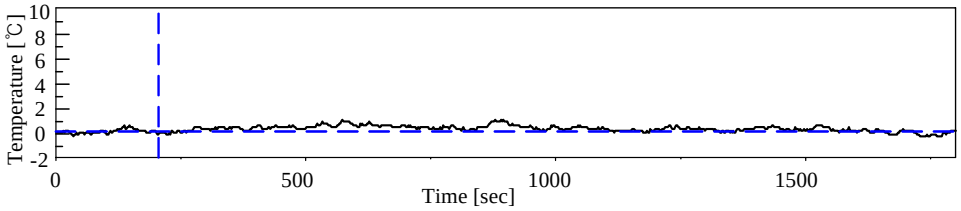

(a) The response of chamber temperature

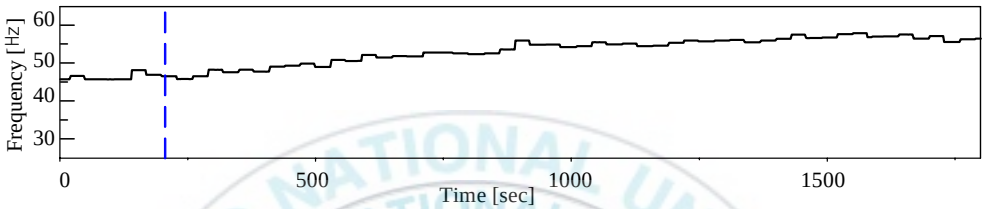

(b) The compressor frequency

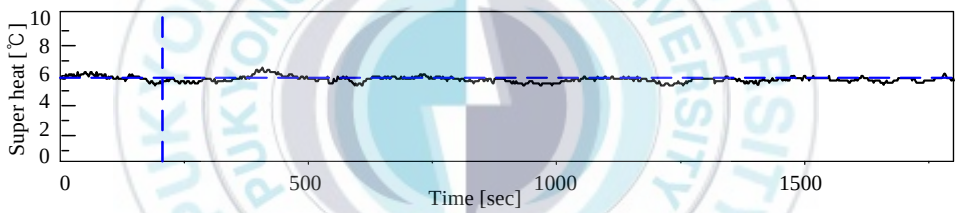

(c) The response of superheat

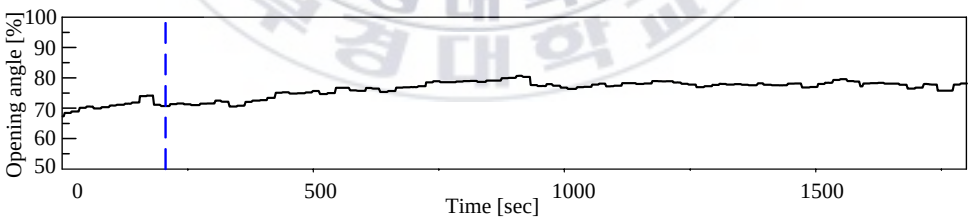

(d) The opening angle of EEV

Fig. 3.9 The responses of chamber temperature and superheat by PI control with feedforward compensator according to the variation of thermal load($T_a^* = 0^\circ C$, $SH^* = 6^\circ C$, $Q = 1.44$ ㎾→1.57 ㎾).

3.1.5 Analysis of the sensitivity of the decoupling model using PI controller with feedforward compensator

To confirm the unreliability of decoupling model how to affect the control performance of PI control with feedforward compensator, the analysis of the sensitivity is studied when the parameters of chamber temperature and superheat model have ±10% errors respectively. In this analysis the proportional gain K_{p1} is 800, integral gain K_{i1} is 0.2, and the gains K_{p2}, K_{i2} are 12 and 0.4. Here, the chamber temperature reference is varied from 4℃ to 0℃.

Fig. 3.10 shows the PI control response with feedforward compensator when the DC gain of chamber temperature model has ±10% errors. The simulation results present that the DC gain errors affect the settling time and the control reference(compressor frequency) is varied with DC gain errors to control the chamber temperature. The superheat control response is changed with the compressor frequency variation. Thus, the DC gain errors of chamber temperature model affect the settling time and do not influence on the steady state.

Fig. 3.11 indicates the PI control response with feedforward compensator when the time constant of chamber temperature model has ±10% errors. The simulation results describe that the time constant errors of chamber temperature model have effect on the rising time of chamber temperature and superheat.

Fig. 3.12 and Fig. 3.13 represent the PI control response with feedforward compensator when the DC gain and time constant of superheat model has ±10% errors respectively. The simulation results show that the parameter errors of superheat have not effect on the chamber temperature because the transfer function G_{2_Ta} is ignored. The parameter errors have very small effect on the superheat control response. The influence of time delay of superheat model does not considered because the error of time delay have little effect on the step response of superheat(see Fig. 2.14).

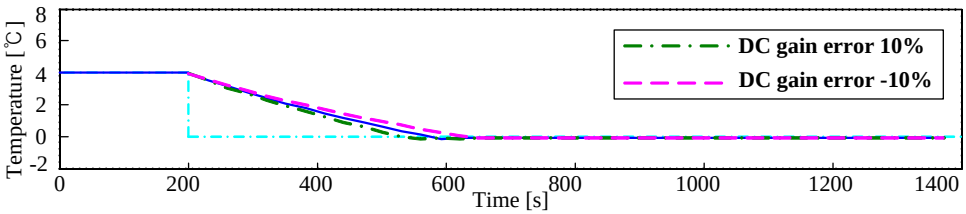

(a) The response of chamber temperature

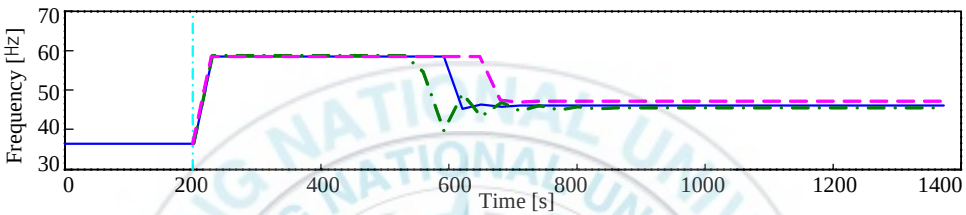

(b) The compressor frequency

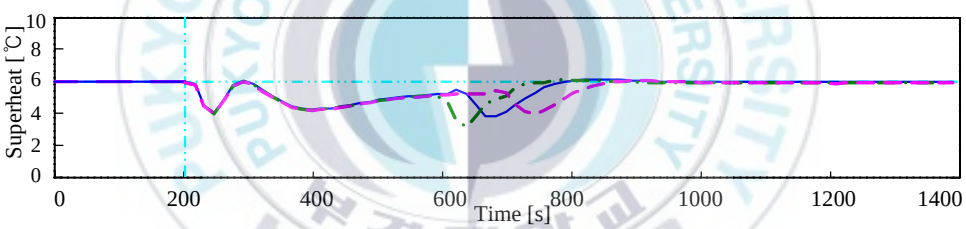

(c) The response of superheat

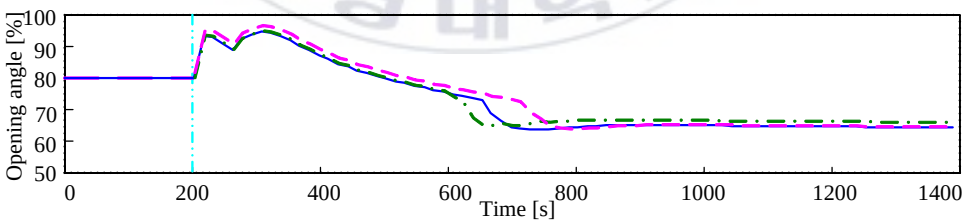

(d) The opening angle of EEV

Fig. 3.10 Analysis of the sensitivity of PI controller when the chamber temperature model has ±10% DC gain error

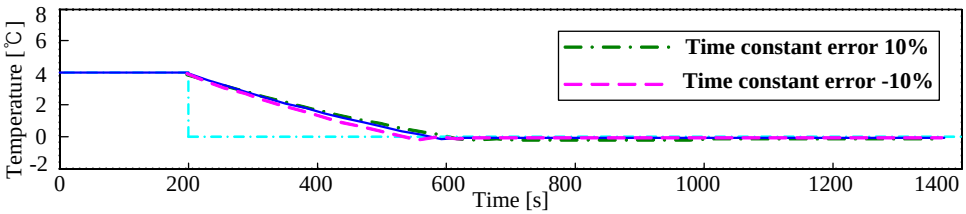

(a) The response of chamber temperature

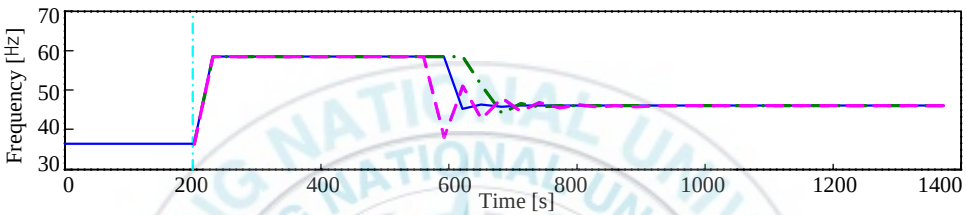

(b) The compressor frequency

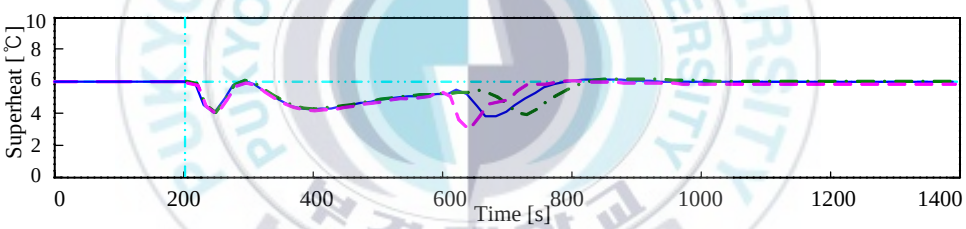

(c) The response of superheat

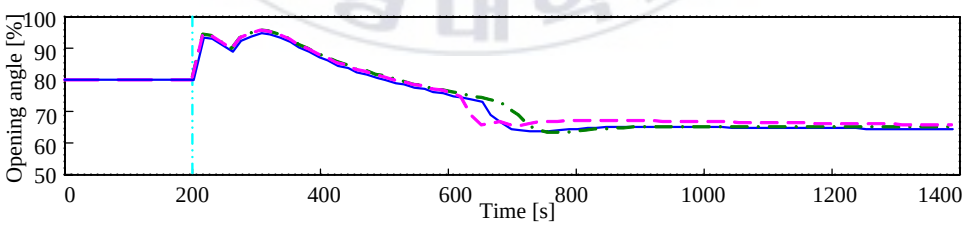

(d) The opening angle of EEV

Fig. 3.11 Analysis of the sensitivity of PI controller when the chamber temperature model has ±10% time constant error

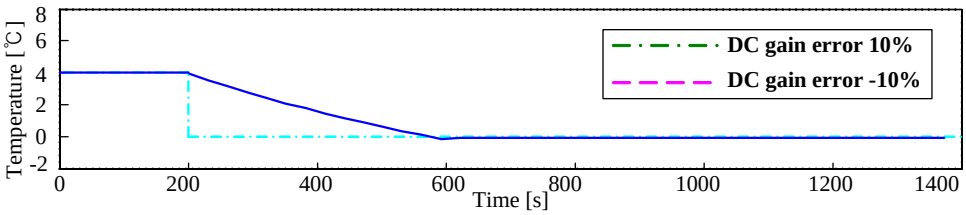

(a) The response of chamber temperature

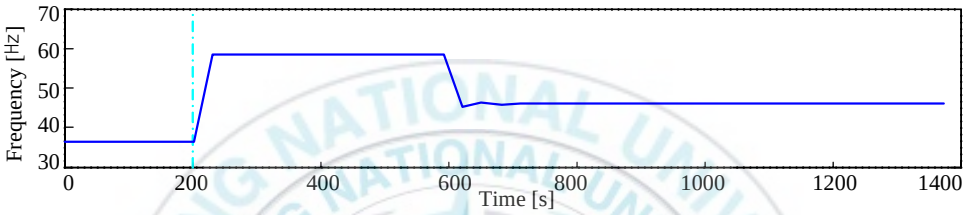

(b) The compressor frequency

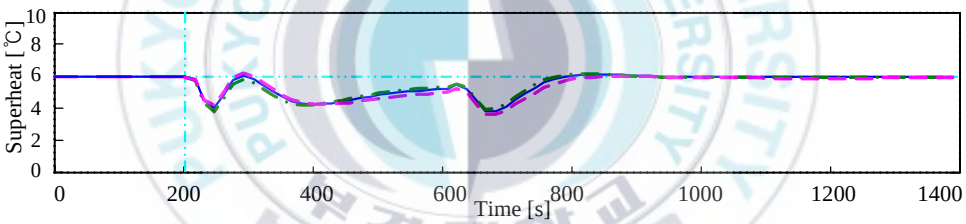

(c) The response of superheat

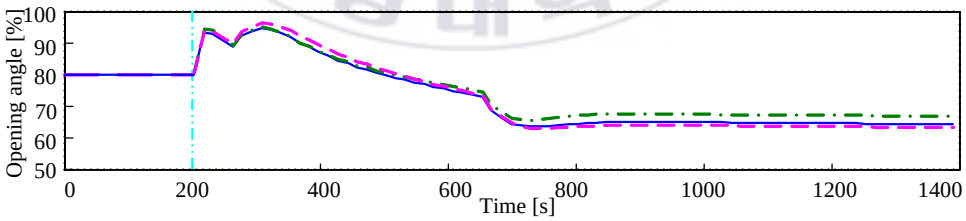

(d) The opening angle of EEV

Fig. 3.12 Analysis of the sensitivity of PI controller when the superheat model has ±10% DC gain error

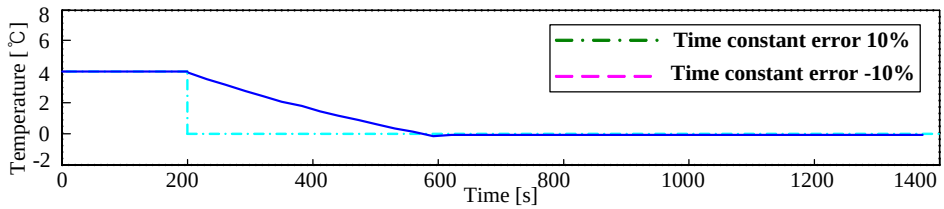

(a) The response of chamber temperature

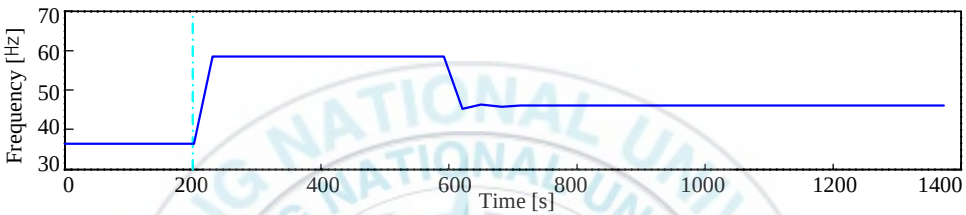

(b) The compressor frequency

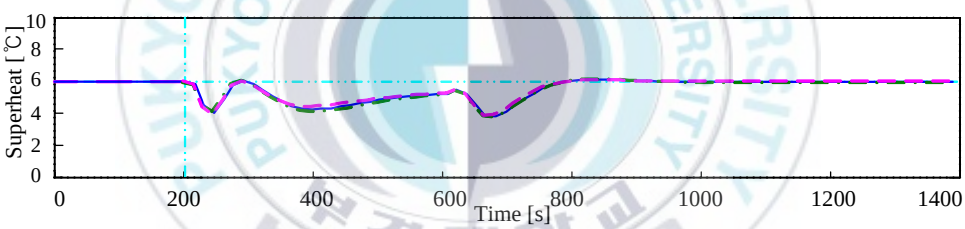

(c) The response of superheat

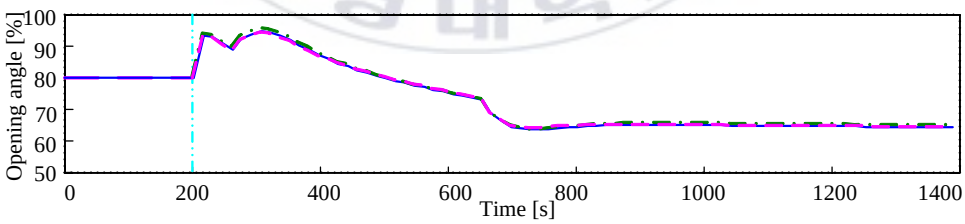

(d) The opening angle of EEV

Fig. 3.13 Analysis of the sensitivity of PI controller when the superheat model has ±10% time constant error

3.1.6 Summation of PI control

In this chapter, the PI controller scheme with decoupling model has been presented to control the thermal capacity and superheat independently for saving energy and progress of COP. The general PI controller without interfering loops inside has been successfully designed and extensive experimental results show that the presented PI controller with the feedforward compensator is effective methods of controlling the VSRS. Key conclusions can be made as follows:

(1) The superheat is controlled as 6℃ within ±1℃ errors even if the chamber temperatures are varied.

(2) The chamber temperature and the superheat are controlled as their reference values within ±1℃ errors although the thermal loads are varied.

(3) Several experimental results are well consistent with simulation results.

(4) The compressor frequency can be varied under the partial loads to save energy and control the temperature precisely.

(5) The superheat is controlled as a constant value to attain high COP although the compressor frequency is varied.

3.2 Design of Fuzzy controller

3.2.1 Introduction of Fuzzy control

In this part we want to introduce the fuzzy control theory at first. Fuzzy control provides a formal methodology for representing, manipulating, and implementing a human's heuristic knowledge about how to control a system. The fuzzy controller has four main components: (1) The "rule-base" holds the knowledge, in the form of a set of rules, of how best to control the system. (2) The inference mechanism evaluates which control rules are relevant at the current time and then decides what the input to the plant should be. (3) The fuzzification interface simply modifies the inputs so that they can in interpreted and compared to the rules in the rule-base. (4) The defuzzification interface converts the conclusions reached by the inference mechanism into the inputs to the plant[54].

To design the fuzzy controller, the control engineer must gather information on how the artificial decision maker should act in the close-loop system. Sometimes this information can come from a human decision maker who performs the control task, while at other times the control engineer can come to understand the plan dynamics and write down a set of rules about how to control the system without outside help.

Fuzzy control system design essentially amounts to (1) choosing the fuzzy controller inputs and outputs, (2) choosing the preprocessing that is needed for the controller inputs and possibly postprocessing that is needed for the outputs, and (3) designing each of the four components of the fuzzy controller.

Using the introduced fuzzy control theory, we will describe the process of fuzzy control design in the concrete at next part.

3.3.2 Design of fuzzy controller

Fig. 3.14 shows a basic composition of fuzzy controller. It is basically consisted of fuzzy rule base, fuzzy inference unit, fuzzification interface,

and defuzzification interface part. The fuzzy rule base(a set of If-Then rules), which contains a fuzzy logic quantification of the expert's linguistic description of how to achieve good control. The fuzzy inference, which emulates the expert's decision making in interpreting and applying knowledge about how best to control the plant. The fuzzification interface, which converts controller inputs into information that the inference mechanism can easily use to activate and apply rules. The defuzzification interface, which converts the conclusions of the inference mechanism into actual inputs for the process.

The fuzzy system has inputs and outputs. The inputs and outputs are "crisp"-that is, they are real numbers, not fuzzy sets. The fuzzification block converts the crisp inputs to fuzzy sets, the inference mechanism uses the fuzzy rules in the rule-base to produce fuzzy conclusions, and the defuzzification block converts these fuzzy conclusions into the crisp outputs. A "linguistic description' will be used to specify rules for the rule-base; hence, linguistic expressions are needs for the inputs and outputs and the characteristics of the inputs and outputs. The linguistic variables are used to describe the fuzzy system inputs and outputs; the linguistic values are used to describe characteristics of the variables.

Fig. 3.15 describes the schematic diagram of refrigeration control system in this paper. Controlled variables in this system are the chamber temperature T_a and the superheat SH which is the difference between the refrigerant temperature at outlet and inlet of an evaporator. The controlled system is the basic refrigeration cycle, and the actuators of the cycle are the induction motor driven by an inverter to control compressor speed and the stepping motor to control the opening angle of EEV The capacity control of the refrigeration system is to adjust refrigerant flow rate by changing compressor speed to cope with thermal load disturbance. On the other hand, the superheat control is to keep up fluctuated superheat as a certain constant value by controlling the opening angle of EEV. To operate the VSRS safely, the operation range of compressor frequency is set as 30㎐~60㎐, and the output value of EEV driver is set as 40~400 step.

Two fuzzy controllers for the capacity and the superheat are designed independently. Input variables for the capacity are made up of ‘e’ and ‘ee’. Here, ‘e’ is the error between reference chamber temperature T_a^* and measured chamber temperature T_a, and also ‘ee’ is rate of the variation of ‘e’ Input variables for the superheat control are also made up ‘e’ and ‘ee’. The output variables are compressor frequency f in the case of the capacity control and the opening angle of EEV VO in the case of the superheat control.

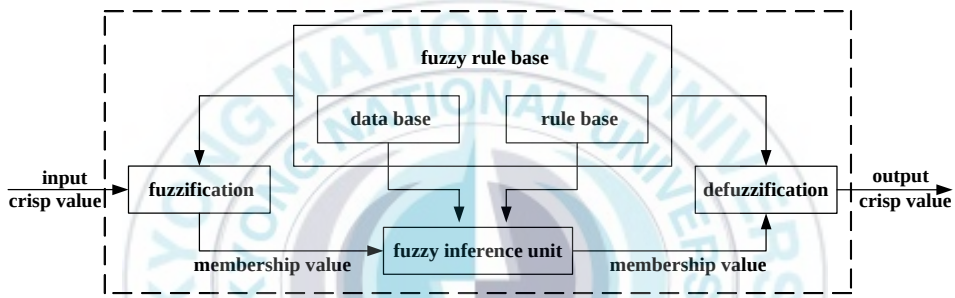

Fig. 3.14 Basic composition of fuzzy control system

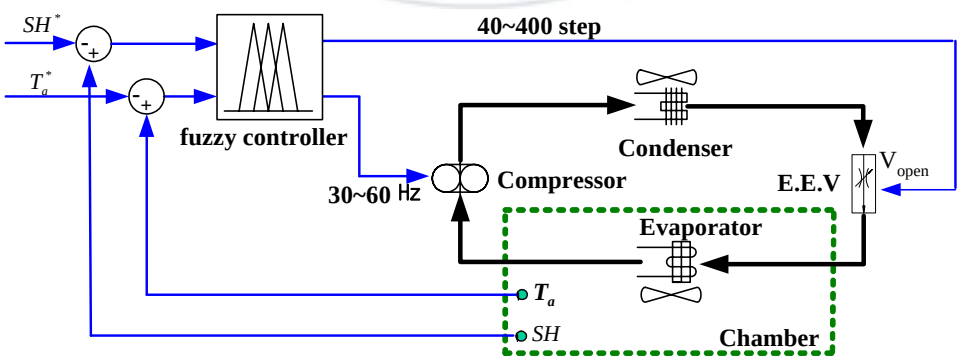

Fig. 3.15 Schematic diagram of the refrigeration system

The rule bases and the membership functions of input and output variable must be determined to design fuzzy controller. In this paper, these are decided by a trial and error manner throughout some experiments. The rule-base captures the expert's knowledge about how to control the plant. The rule-base of fuzzy controller holds the linguistic variables, linguistic values, their associated membership functions, and the set of all linguistic rules. The mapping of the inputs to outputs for the fuzzy system is in part characterized by If-Then form. Table 3.2 and Table 3.3 show fuzzy rule bases for controlling the capacity and the superheat. The rule bases were decided from the experience of the controller designer and several experiments.

The membership functions are subjectively specified in and ad hoc manner from experience or intuition. There are some types of membership function such as triangle form and trapezoidal form etc. The triangle membership function was used to produce a rule base for fuzzy control in this paper. Because the triangle membership function is the most wildly used in the fuzzy control field and it is very easy to design fuzzy controller. The triangle membership function is used for conversion between crisp and membership value. Fig. 3.16 and Fig. 3.17 are membership functions for the capacity control and the superheat control respectively. The range of the capacity and superheat of 'e' were -3~3℃. The range of 'ee' in the superheat was smaller than the capacity. The control output range of the capacity was -20~20㎐ and the range of the superheat control was -9~6%.

Output is calculated in a fuzzy inference part using the fuzzy rule bases. The fuzzy inference has two basic tasks: (1) determining the extent to which each rules is relevant to the current situation as characterized by the inputs; and (2) drawing conclusions using the current inputs and the information in the rule-base. This inference is based on the Mamdani min-max arithmetic.

In the defuzzification part, the defuzzification operates on the implied fuzzy sets produced by the inference mechanism and combines their effects to provide the most certain controller output. Some think of defuzzification as decoding the fuzzy set information produced by the inference process into numeric fuzzy controller outputs. The center of gravity(COG)

defuzzification method for combining the recommendations represents by the implied fuzzy sets from all the rules. The membership value is converted to a crisp value as final output, and the crisp value is chosen using the center of area and area of each implied fuzzy set, and is given by

$$U^{crisp} = \frac{\sum \mu(i) b_i}{\sum \mu(i)} \tag{3-13}$$

Where, U^{crisp} means crisp output of fuzzy inference, b_i indicates center of area of a membership function and μ_i is the output of fuzzy inference. Notice that COG can be easy to compute since it is often easy to find the area under a membership function.

Table 3.2 Rule base for capacity control

		ee						
		NB	NM	NS	Z	PS	PM	PB
	NB	NB	NB	NB	NB	Z	Z	Z
	NM	NB	NB	NM	NM	Z	Z	Z
	NS	NB	NM	NS	NS	Z	Z	Z
e	Z	NM	NS	Z	Z	Z	Z	Z
	PS	NS	Z	Z	Z	PS	PM	PB
	PM	Z	Z	Z	PS	PM	PB	PB
	PB	Z	Z	Z	PB	PB	PB	PB

Table 3.3 Rule base for superheat control

		ee						
		NB	NM	NS	Z	PS	PM	PB
	NB	NB	NB	NM	NM	NS	Z	Z
	NM	NB	NM	NS	NS	Z	Z	Z
	NS	NM	NS	NS	Z	Z	Z	Z
e	Z	NM	NS	Z	Z	Z	Z	Z
	PS	NS	Z	Z	Z	PS	PM	PB
	PM	Z	Z	Z	PS	PS	PM	PB
	PB	Z	Z	Z	PS	PM	PB	PB

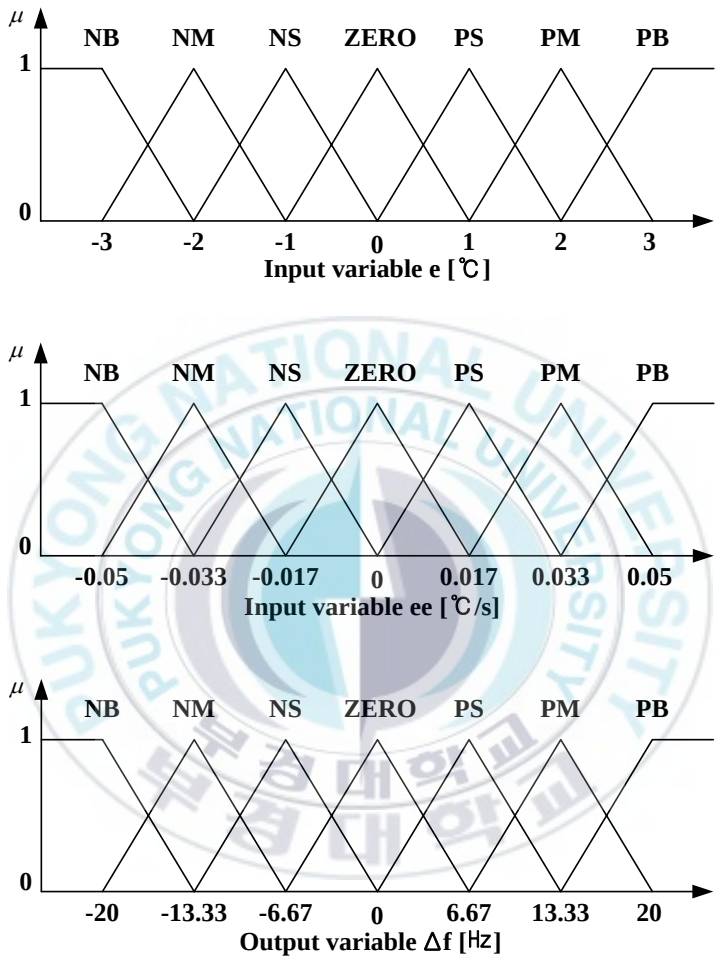

Fig. 3.16 Membership function for capacity control

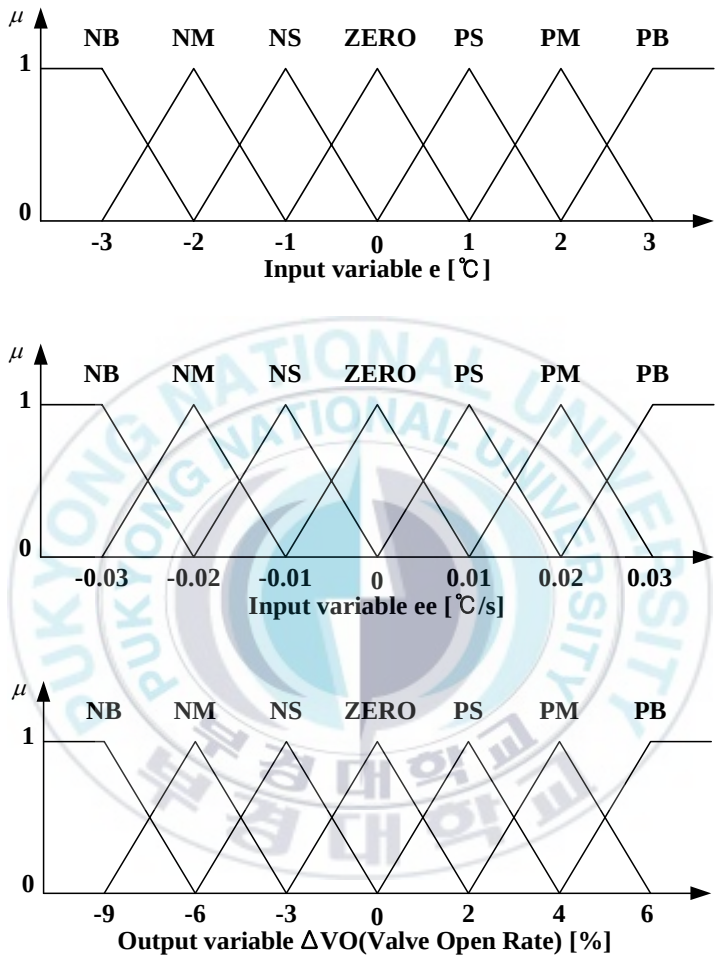

Fig. 3.17 Membership function for superheat control

3.2.3 Experimental result of fuzzy control and discussion

Photo. 3.1 shows real experimental system. Fuzzy controller for controlling both capacity and superheat is realized by the Programmable Logic Controller(PLC) with specific converter modules D/A and TC(Thermocouple). Table 3.1 represents the specification of a test unit of the experimental system. The experimental system was composed of basic refrigeration cycle and control system. The main components of the control system were an inverter, a step valve control interface and the PLC. The compressor was driven by the 3 phase induction motor with a general V/f constant type inverter. The stepper motor to drive EEV was operated by a step valve control interface. The input control signals of inverter and step valve control interface were gotten from D/A unit of the PLC. All temperatures were measured by thermocouples(T-type). The temperature information was transmitted to TC unit of the PLC with real time for operating input variables, ‘e’ and ‘ee’, in the fuzzy controller. The control sampling time was set at 30 seconds in this study.

Fig. 3.18 shows control responses of the chamber temperature and the superheat when the chamber temperature reference was abruptly changed from 4℃ to 2℃. The thermal load was 1.5㎾ and the superheat control reference was set at 6℃. From the experimental results, the chamber temperature response was fairly good but the superheat oscillated and settling time was very long. It is desirable to control the capacity and superheat simultaneously in the variable speed refrigeration system. In spite of simultaneous control of them, good control performances can not be obtained because of the effect of interference of the variation of compressor speed toward superheat. The evaporating pressure will be varied when the compressor frequency is varied. Then the superheat of evaporator is also changed due to the variation of evaporating pressure. To overcome this problem, we proposed fuzzy control with feedforward compensator of superheat which can eliminate the influence of the interfering loop between capacity and superheat.

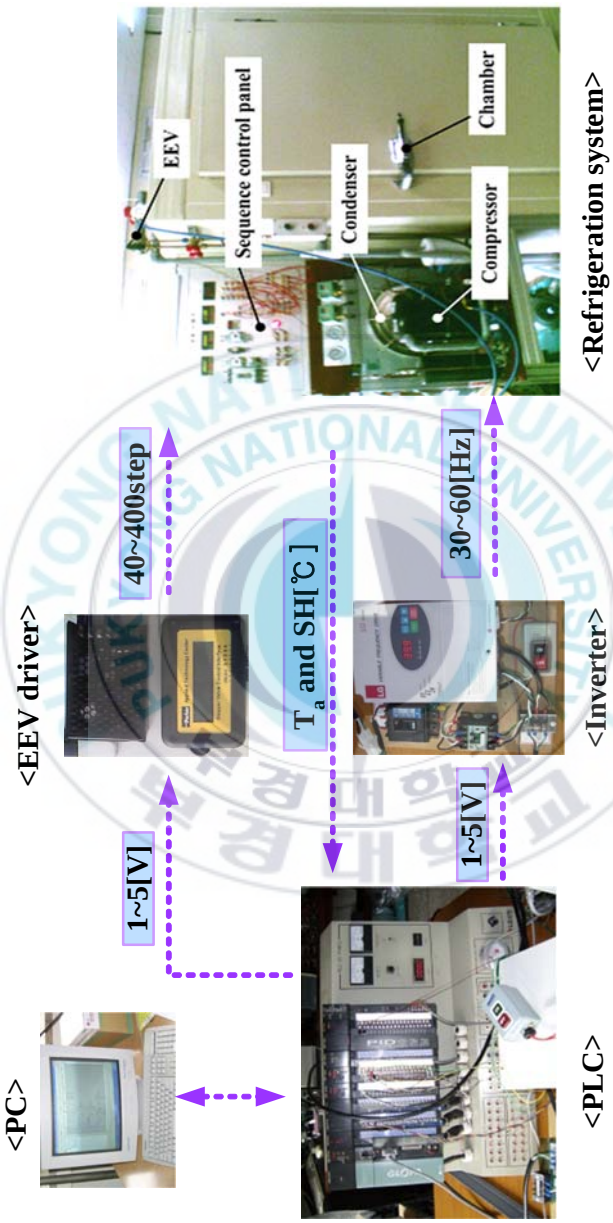

Photo. 3.1 Experimental system of fuzzy control for capacity and superheat control

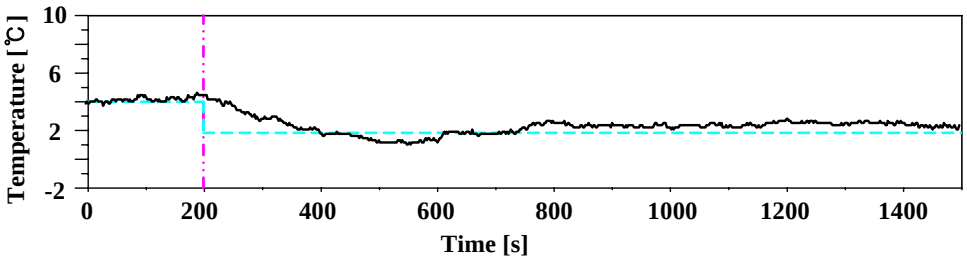

(a) The response of chamber temperature

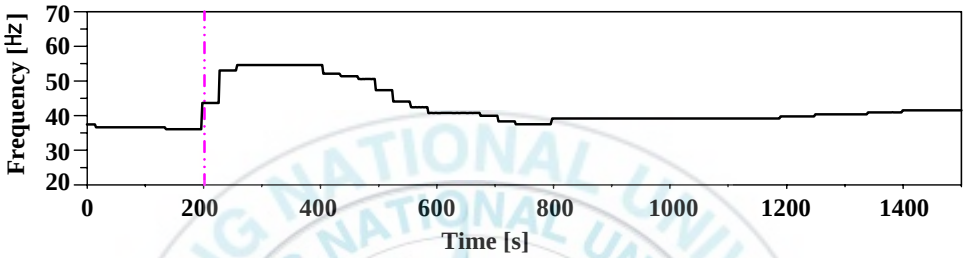

(b) The compressor frequency

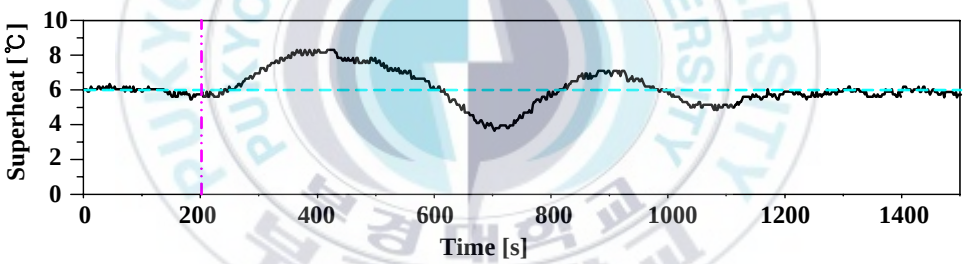

(c) The response of superheat

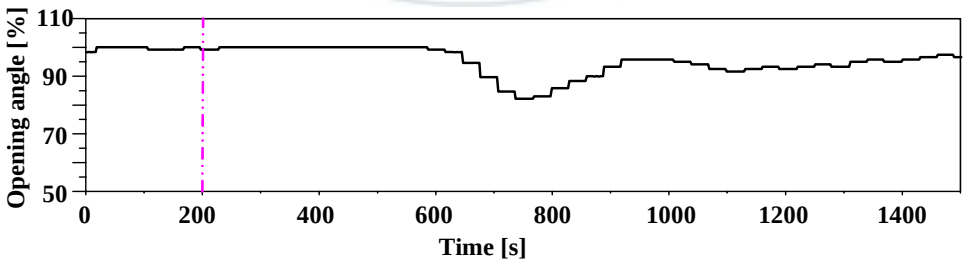

(d) The opening angle of EEV

Fig. 3.18 The responses of chamber temperature and superheat by fuzzy control according to the variation of chamber temperature reference($T_a^* = 4^\circ C \rightarrow 2^\circ C$, $SH^* = 6^\circ C$, $Q = 1.5$ ㎾).

3.2.4 Design of the fuzzy controller with feedforward compensator

Fig. 3.19 indicates feedforward compensator of superheat. Disturbance d which has an effect on superheat due to the variation of compressor speed Δf can be expressed as Eq. (3-14).

$$d = \Delta SH = \frac{\Delta SH}{\Delta f}\Delta f \tag{3-14}$$

To cancel the effect of this disturbance, we designed the compensator such as Eq. (3-15) by an iteration method.

$$u_f = kd = k'\Delta f \tag{3-15}$$

Where, u_f is compensating quantity of ΔVO, and k' was set as 0.5 in this paper.

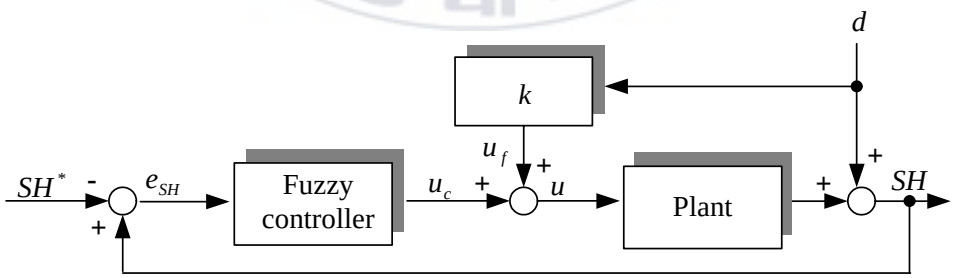

Fig. 3.19 Schematic diagram of feedforward compensator of superheat control

3.2.5 Experimental result of fuzzy control with feedforward compensator and discussion

Fig. 3.20 describes responses of chamber temperature and superheat based on the fuzzy control with the feedforward compensator. The experimental conditions were the same as previous experiment in Fig. 3.18. Fig. 3.20(a) shows response of chamber temperature by the fuzzy control with the compensator when the chamber temperature reference was varied abruptly at the time of 200 second. It takes about 400 seconds from reference change to get close set point value. Fig. 3.20(b) shows the response of compressor frequency to follow the reference of chamber temperature. It can be seen that the compressor set point frequency for controlling the capacity was very stable. Fig. 3.20(c) presents the response of superheat control according to the change of chamber temperature reference. The superheat must be controlled as a constant value, 6℃, even the compressor speed and chamber temperature were varied. The percent overshoot is observed 17% approximately in this figure, but the maximum overshoot of the superheat is kept less than 8℃. It is acceptable superheat in this system. Fig. 3.20(d) indicates the opening angle of EEV when the fuzzy controller was operated. The opening angle of EEV was adjusted with stable to maintain the superheat as 6℃. These experimental results provide fairly good control performances of capacity and superheat when the chamber temperature reference was varied.

Fig. 3.21 describes responses of chamber temperature and superheat when thermal load was abruptly varied from 1.35㎾ to 1.57㎾ at 200 second. The chamber temperature reference was set at 2℃ and the superheat reference was 6℃. From Fig. 3.21(a), found that the chamber temperature was maintained as 2℃ even the thermal load was varied. Fig. 3.21(b) shows that the compressor frequency increased to control the chamber temperature as 2℃ because of the increase of thermal load. Fig. 3.21(c) presents the fuzzy control response of superheat according to the change of thermal load. The superheat has been controlled as a constant value, 6℃, to obtain high

COP. Fig. 3.21(d) shows the opening angle of EEV under the given thermal load. The fuzzy control responses indicate good control performance of the capacity and superheat under various thermal load conditions.

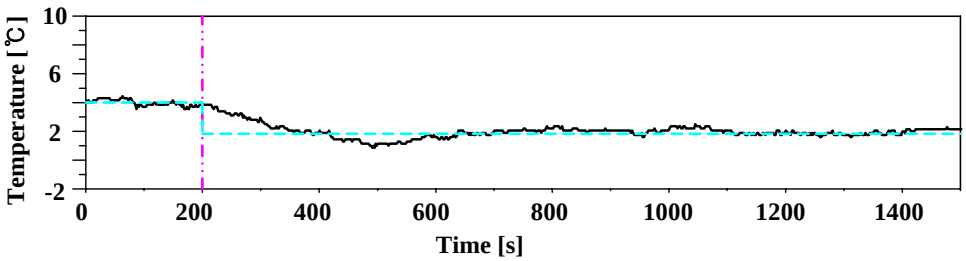

(a) The response of chamber temperature

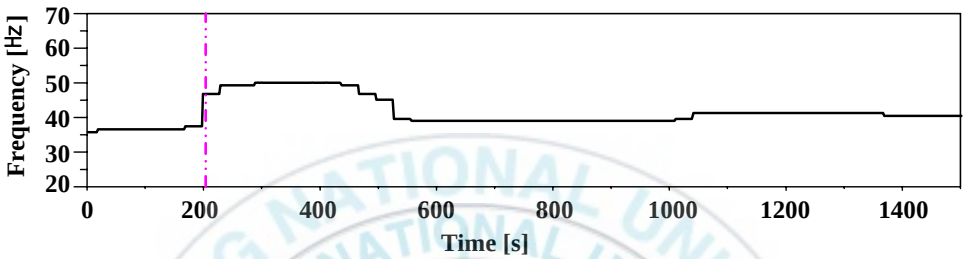

(b) The compressor frequency

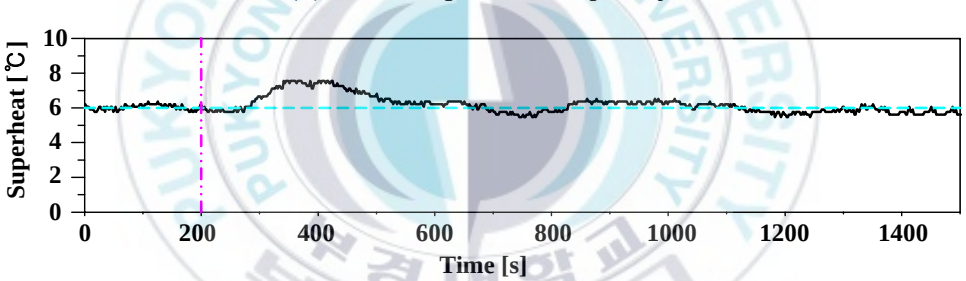

(c) The response of superheat

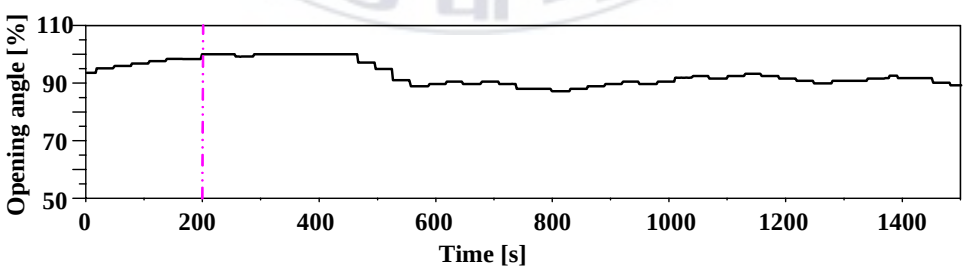

(d) The opening angle of EEV

Fig. 3.20 The responses of chamber temperature and superheat by fuzzy control with feedforward compensator according to the variation of chamber temperature reference($T_a^* = 4^\circ C \rightarrow 2^\circ C$, $SH^* = 6^\circ C$, $Q = 1.5$ ㎾).

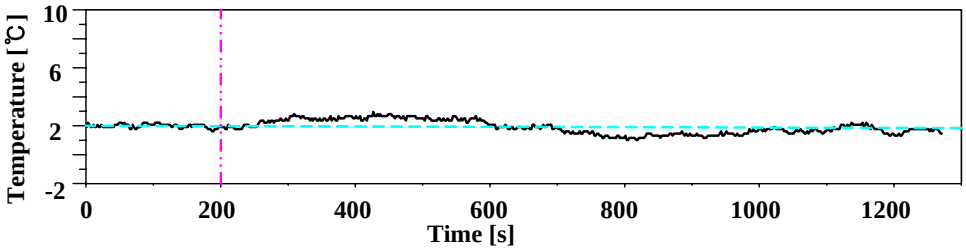

(a) The response of chamber temperature

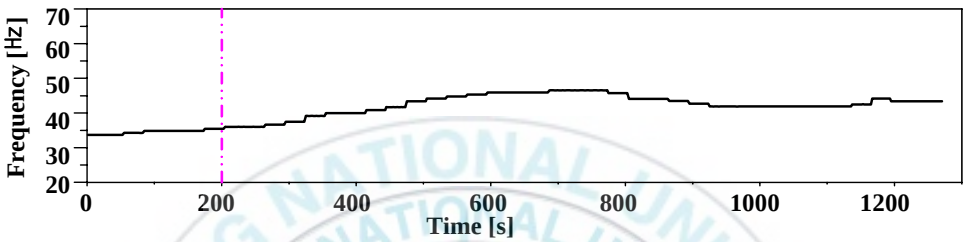

(b) The compressor frequency

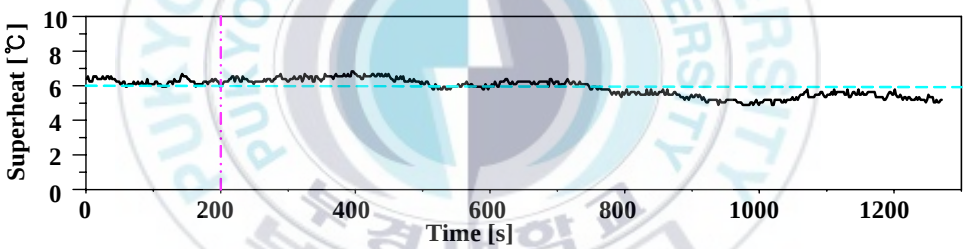

(c) The response of superheat

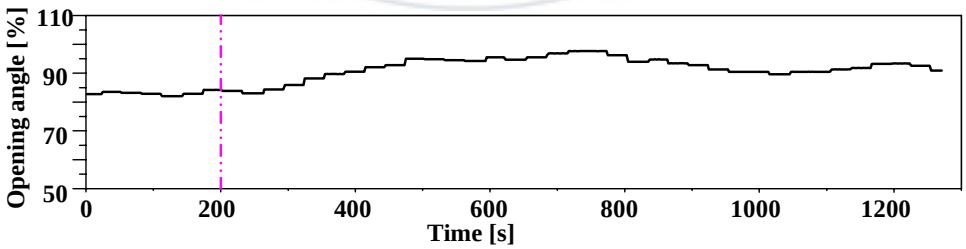

(d) The opening angle of EEV

Fig. 3.21 The responses of chamber temperature and superheat by fuzzy control with feedforward compensator according to the variation of thermal load($T_a^* = 2^\circ C$, $SH^* = 6^\circ C$, $Q = 1.35$ ㎾→1.57 ㎾).

3.2.6 Summation of fuzzy control

In this chapter, we suggest fuzzy control with feedforward compensator of superheat to progress both energy saving and coefficient of performance(COP) in VSRS. By adopting the fuzzy control, the controller design for the capacity and superheat is possible without depending on a dynamic model of the system. Moreover, the feedforward compensator of the superheat can eliminate influence of the interfering loop between capacity and superheat, and the capacity and superheat are controlled simultaneously and independently. Key conclusions can be made as follows:

(1) The input parameter 'ee' is very important design factor as well as 'e' to get good control performance in the capacity and superheat control design.

(2) The superheat response is very sensitive to the variance of compressor speed. Thus, good control performance hardly expected by conventional basic fuzzy controller without compensation of the influence of the compressor speed change.

(3) Fairly good control performances were established by the fuzzy controller with feedforward compensator of the superheat. The simultaneous control of chamber temperature and superheat based on the suggested controller had good transient responses even though the references and thermal load were varied.

3.3 Analysis of the control performance in PI control and fuzzy control

The PI control logic and fuzzy control algorism have their merits and faults respectively when design the controller.

(1) The control performance of PI control is better than fuzzy control when it has very precise mathematical dynamic models, but it is not easy to obtain precise dynamic model, which is the shortcoming of PI controller.

(2) The fuzzy control performance can be also got nearly equivalent to the PI control without dynamic model, and it is the main advantage of fuzzy control algorism. But when it has more suitable membership function and rule base, better control performance can be obtained.

Chapter 4

Conclusions

In this thesis, the decoupling model and independent control method has been presented to control the VSRS for progressing COP. For the purpose of this, we proposed decoupling model for controlling the capacity and degree of superheat independently, designed PI controller with decoupling model and fuzzy control without dynamic model. Key conclusions can be made as follows:

(1) The empirical decoupling models to control capacity and superheat are expressed as a simple first-order system with time delay. They are obtained several experiments under various operating conditions.

(2) The test results strongly indicate that the proposed models are conveniently employed to formulate a robust control algorithm for regulating the VSRS. It has been confirmed by both theoretically and experimentally that the decoupling models is definitely practical for controlling the VSRS under variable operating conditions.

(3) In addition, the overall control system without interfering loops is primarily designed to achieve precise control objective and improve COP for the VSRS.

(4) Then, the general PI controller without interfering loops has been successfully designed. Extensive experimental results show that the presented PI controller with the feedforward compensator is effective methods for controlling the VSRS.

(5) The decoupling PI control can offer the improved system performance, by not only controlling chamber temperature precisely but also guaranteeing high COP level in the VSRS.

(6) The fuzzy controller proposed in this paper aimed at simultaneous control of the capacity and superheat without troublesome dynamic model of the system.

(7) Some experiments are conducted to design the appropriate fuzzy controller by an iteration manner. We investigated important design factors effect on control performance after design of the fuzzy controller. Especially, we found that the fuzzy controller with feedforward compensator of the superheat can obtain good transient response.

(8) Some control experimental results show that the proposed fuzzy controller is suitable for the capacity and the superheat control of the variable speed refrigeration system. The fuzzy control with feedforward compensator for the capacity and superheat attained to the purpose of progressing COP in the VSRS.

(9) We can get nearly equivalent control performance to that of PI controller by using the fuzzy controller; it will be very useful design methodology for engineers in the industrial fields.

Reference

[1] Y.T. Lee, Y.C. Kim, M.S. Kim, 1996, Performance of an inverter refrigeration system with a change of expansion devices. Journal of SAREK, Vol. 11, No. 6, pp. 928-936.

[2] J.D. Kim, H.K. Oh, J.I. Yoon, 1995, A study on dynamic characteristics of a refrigeration system by controlling the evaporator superheat, Journal of KSME, Vol. 19, No. 8, pp. 2012-2021.

[3] C. Aprea, F. de Rossi, A. Greco, C. Renno, 2003, Refrigeration plant exegetic analysis varing the compressor capacity, International Journal of Energy Research, Vol. 27, pp.653-669.

[4] C. Aprea, C. Renno, 2004, An experimental analysis of a thermodynamic model of a vapor compression refrigeration plant on varying the compressor speed, International Journal of Energy Research, Vol. 28, pp. 537-549.

[5] J.M. Choi, Y.C. Kim, J.H. Ha, 2001, Performance of the flow distribution and capacity modulation of a multi-heat pump system, Journal of SAREK, Vol. 13, No. 5, pp. 313-320.

[6] B.H. Kim, 2001, An experimental investigation on the variation of heating performance due to the refrigeration flow control in a variable-speed heat pump, Journal of SAREK, Vol. 13, No. 8, pp. 746-756.

[7] J.M. Choi, Y.C. Kim, 2003, Capacity modulation of an inverter-driven multi-air conditioner using electronic expansion valves, Journal of Energy, Vol. 28, pp. 141-155.

[8] S.O. Choi, J.H. Kim, H.S. Yang, J.S. Kim, 1994, Study on control of refrigeration flow rate and characteristics of superheat in evaporator using electronic expansion valve, Journal of SAREK, Vol. 6, No. 4, pp. 380-387.

[9] J.M. Choi, Y.C. Kim, 2002, Superheat control of an inverter-driven heat pump using PI control algorithm, International Journal of Air-conditioning and Refrigeration, Vol. 10, No. 2, pp. 106-115.

[10] W. Chen, Z.J. Chen, R.Q. Zhu, Y.Z. Wu, 2002, Experimental investigation of a minimum stable superheat control system of an evaporator, International Journal of Refrigeration, Vol. 25, pp. 1137-1142.

[11] Donal P. Finn, 2000, Control and optimization issues associated with algorithm-controlled refrigeration throttling devices, ASHRAE, Vol. 106, No. 1, pp. 1-10.

[12] H.S. Yang, H.S. Kim, J.H. Kim, S.B. Kim, J.S. Kim, 1993, Control of refrigeration compressor capacity using inverter, Journal of SAREK, Vol. 5, No. 2, pp. 94-101.

[13] Y.C. Park, M.K. Kim, 1997, A study of frequency control of an inverter heat pump for indoor air temperature adjustment, Journal of KSME, Vo. 21, No. 10, pp. 1262-1272.

[14] D.S. Jung, M.S. Kim, M.S. Kim, W.Y. Lee, 2000, Capacity modulation of a multi-type heat pump system using PI control, Journal of SAREK, Vol. 12, No. 5, pp. 466-475.

[15] D.S. Jung, M. Kim, M.S. Kim, 1999, PID control of multi-type heat pump system, Autumn proceeding of SAREK, pp. 541-545.

[16] M. Willatzen, N.B.O.L. Pettit, L. Ploug Sorensen, 1998, A general dynamic simulation model for evaporators and condensers in refrigeration. Part Ⅰ: Moving-boundary formulation of two-phase flows with heat exchange, International Journal of Refrigeration, Vol. 21, No. 5, pp. 398-403.

[17] M. Willatzen, N.B.O.L. Pettit, L. Ploug Sorensen, 1998, A general dynamic simulation model for evaporators and condensers in refrigeration. Part Ⅱ: Simulation and control of an evaporator, International Journal of Refrigeration, Vol. 21 No. 5, pp. 404-414.

[18] Gisbert Stoyan, 1994, A dynamical model adequate for controlling the evaporator of a heat pump, Rev. Int. Froid., Vol. 17, No. 2, pp. 101-108.

[19] H. Wang, S. Touber, 1991, Distributed and non-steady-state modeling of an air cooler, International Journal of Refrigeration, Vol. 14, No. 3, pp. 98-111.

[20] C. Aprea, C. Renno, 1999, An air cooled tube-fin evaporator model for an expansion valve control law, Mathematical an computer modeling, Vol. 30, pp. 135-146.

[21] J.D. Kim, J.I. Yoon, K. Higuchi, 1996, Analysis of dynamic characteristics on condenser for the control of air conditioning systems, Journal of SAREK, Vol. 8, No. 3, pp. 386-396.

[22] J.D. Kim, J.I. Yoon, Y.S. Kim, C.G. Moon, 2001, Analysis of characteristics on small Air-conditioning type evaporator, Journal of KOSME, Vol. 25, No. 3, pp. 573-580.

[23] J.P. Lee, J.D. Kim, J.I. Yoon, 1998, Dynamic characteristics analysis of fin coil type evaporator, Autumn proceeding of the SAREK, pp. 752-758.

[24] Y.G. Shin, S.Cho, C.S. Tea, C.Y. Jang, 2007, A dynamic simulation model of electronic-expansion-valve-controlled evaporator, Journal of SAREK, Vol. 19, No. 2, pp. 183-190.

[25] K. Bourouni, M. T. Chaibi, 2004, Modeling of heat and mass transfer in a horizontal-tube falling film condenser for brackish water desalination in remote areas, Journal of Desalination, Vol. 166, pp. 17-24.

[26] John Judge, Reinhard Radermacher, 1997, A heat exchanger model for mixtures and pure refrigerant cycle simulations, International Journal of Refrigeration, Vol. 20, No. 4, pp. 244-255.

[27] P. Mithraratne, N.E. Wijeysundera, 2001, An experimental and numerical study of the dynamic behavior of a counter-flow evaporator, International Journal of Refrigeration, Vol. 24, pp. 554-565.

[28] X. Jia, C.P. Tso, P. Jolly, Y.W. Wong, 1999, Distributed steady and dynamic modeling of dry-expansion evaporators, International Journal of Refrigeration, Vol. 22, pp. 126-136.

[29] P. Mithraratne, N.E. Wijeysundera, T.Y. Bong, 2000, Dynamic simulation of a thermostatically controlled counter-flow evaporator, International Journal of Refrigeration, Vol. 23, pp. 174-189.

[30] R.N.N. Koury, L. Machado, K.A.R. Ismail, 2001, Numerical simulation of a variable speed refrigeration system, International Journal of

Refrigeration, Vol. 24, pp. 192-200.

[31] Andrew G. Alleyne, 2004, Dynamic modeling and control of multi-evaporator Air-conditioning systems, ASHRAE, Vol. 110, No. 1, pp. 109-119.

[32] Zhao Lei, M. Zaheeruddin, 2005, Dynamic Simulation and Analysis of a Water Chiller Refrigeration System, Applied Thermal Engineering, Vol. 25, pp. 2258-2271.

[33] G.L.Morini, S.Piva, 2007, The Simulation of Transients in Thermal Plant Part Ⅰ: Mathematical Model, Applied Thermal Engineering, Vol. 27, pp. 2138-2144.

[34] H.B Jiang, Reinhard Radermacher, 2003, A distributed model of a space heat pump under transient conditions, Int. J. Energy Res., Vol. 27, pp. 145-160.

[35] T.S. Kim, K.S. Hong, H.C. Sohn, 2001, Evaporator superheat control of a Multi-type Air-conditioning/refrigeration system, Energy Engg. J., Vol. 10. No. 3, pp. 253-265.

[36] G.B Lee, K.J. Yoo, M.S. Kim, 2005, Analysis of the steady state and transient characteristics of a multi-type refrigeration system, Autumn proceedings of the SAREK, pp. 439-444.

[37] C.P. Underwood, 2001, Analyzing multivariable control of refrigeration plant using matlab/simulink, Seventh International IBPSA Conference, pp. 287-294.

[38] A. Outtagarts, P. Haberschill, M. Lallemand, 1997, The transient response of an evaporator fed through an electronic expansion valve, International Journal of Energy Research, Vol. 21, pp. 793-807.

[39] C. Aprea, C. Renno, 2001, Experimental analysis of a transfer function for an air cooled evaporator, Applied Thermal Engineering, Vol. 21, pp. 481-493.

[40] J.M. Choi, Y.C. Kim, J.H. Ha, 2001, Experimental study on superheat control of a variable speed heat pump, Journal of SAREK, Vol. 13, No. 4, pp. 233-241.

[41] S.H. Yoon, H.W. Chang, 2001, Empirical modeling and control

performance simulation of an inverter heat pump system, Summer proceedings of the SAREK, pp. 725-730.

[42] D.Y. Han, B.G. Lim, 2000, Dynamic model of the electronic expansion valve for the development of superheat temperature control algorithm, Summer proceedings of the SAREK, pp. 1343-1347.

[43] J.M. Choi, Y.C. Kim, J.H. Ha, 2001, Experimental study on superheat control of a variable speed heat pump, Journal of SAREK, Vol. 13, No. 4, pp. 233-241.

[44] S.H. Yoon, H.W. Chang, 2001, Characteristic and control performance analysis of a multi-type inverter heat pump system, Summer proceedings of the SAREK, pp. 1339-1345.

[45] D.Y. Han, H.J. Kwon, 2001, Compressor control of a Multi-type Air-conditioning system, Journal of the SAREK, Vol. 13, No. 8, pp. 780-788.

[46] D.Y. Han, H.J. Kwon, 2000, Compressor speed control of the multi-type air conditioning system by using a fuzzy algorithm, Summer proceedings of the SAREK, pp. 1348-1352.

[47] D.Y. Han, H.J. Kwon, 2000, Experimental study on the compressor control of a Multi-type Air-conditioning system, Autumn proceedings of the SAREK, pp. 208-213.

[48] C. Apreaa, R. Mastrullob, C. Rennoa, 2004, Fuzzy Control of the Compressor Speed in a Refrigeration Plant, International Journal of Refrigeration, Vol. 27, pp. 639-648.

[49] J.H. Kim, W.Y. Kim, J.K. Kang, I.S. Jang, J.S. Kim, 1997, Fuzzy control of superheat and evaporating temperature of evaporator in refrigeration and air conditioning system, International Journal of Air-conditioning and Refrigeration, Vol. 5, pp. 185-194.

[50] D.Y. Han, K.J. Park, 2006, Fuzzy control algorithm for the compressor and the electronic expansion valve for a multi-type air-conditioning system using multiple input variables, Journal of the SAREK, Vol. 18. No. 2, pp. 163-171.

[51] Katsuhiko Ogata, 2002, Modern control engineering, Prentice Hall, 4th

edition.

[52] Franklin, G.F., J.D. Powell, M.L. Workman, 1990, Digital control of dynamic system, Addison-Wesley, 2nd edition.

[53] William S. Levine, 1996, The control handbook, CRC Press.

[54] H.B. Verbruggen, H.J. Zimmermann, R. Babuska, 1999, Fuzzy algorithms for control, Kluwer academic publishers.

Publications and conferences

Publications

[1] Li Hua, Seok-Kwon Jeong, 2006, An empirical model for decoupling control of a variable speed refrigeration system, Journal of the Korean Society for Power System Engineering, Vol. 10, No. 3, pp. 81-87.

[2] Li Hua, Seok-Kwon Jeong, Jung-In Yoon, 2006, Decoupling control design for refrigeration system of a ship, Journal of the Korean Society of Marin Engineering, Vol. 30, No. 7, pp. 808-815.

[3] Li Hua, Dong-Woo Lee, Seok-Kwon Jeong, Jung-In Yoon, 2007, Fuzzy control with feedforward compensator of superheat in a variable speed refrigeration system, Journal of the Korean Society of Marin Engineering, Vol. 31, No. 3, pp. 252-262.

[4] Li Hua, Seok-Kwon Jeong, 2007, The control of superheat and capacity for a variable speed refrigeration system based on PI control logic, International Journal of Air-conditioning and Refrigeration, Vol. 15, No. 2, pp. 54-60.

[5] Li Hua, Seok-Kwon Jeong, 2007, Design and analysis of fuzzy control in a variable speed refrigeration system, International Journal of Air-conditioning and Refrigeration, Vol. 15, No. 2, pp. 61-69.

[6] Li Hua, Jeong-Pil Choi, Seok-Kwon Jeong, Joo-Ho Yang, Dong-Gyu Kim, 2007, PI control with the smith predictive controller for a variable speed refrigeration system, International Journal of Air-conditioning and Refrigeration, Vol. 15, No. 3, pp. 129-136.

[7] Li Hua, Seok-Kwon Jeong, Jung-In Yoon, Sam-Sang You, 2008, An empirical model for independent control of variable speed refrigeration system, Applied Thermal Engineering(SCIE), in press.

[8] Li Hua, Seok-Kwon Jeong, Sam-Sang You, 2008, Feedforward control of capacity and superheat for a variable speed refrigeration system, Applied Thermal Engineering(SCIE), accepted.

Conferences

[1] Li Hua, Dong-Woo Lee, Seok-Kwon Jeong, 2005, An experimental model for a variable speed heat pump system, Proceeding of 2005 International Symposium on Advanced Mechanical Engineering(Busan), pp. 122-127.

[2] Li Hua, Dong-Woo Lee, Seok-Kwon Jeong, 2005, A decoupling model for superheat and capacity control of a variable speed refrigeration system, Proceeding of 2005 International Symposium on Advanced Engineering(Busan), pp. 132-140.

[3] Dong-Woo Lee, Li Hua, Seok-Kwon Jeong, 2005, Superheat characteristics for decoupling control of refrigeration system with a variable speed compressor, The Autumn Conference of Korean Society for Power System Engineering, pp. 309-314.

[4] Li Hua, Dong-Woo Lee, Seok-Kwon Jeong, 2006, An empirical model for decoupling control of a variable speed refrigeration system, The Spring Conference of Korean Society for Power System Engineering, pp. 286-291.

[5] Dong-Woo Lee, Li Hua, Seok-Kwon Jeong, 2006, Superheat and Capacity Control of a Variable Speed Refrigeration System by Fuzzy Controller, The Spring Conference of Korean Society for Power System Engineering, pp. 279-285.

[6] Li Hua, Dong-Woo Lee, Seok-Kwon Jeong, 2006, Decoupling control for a variable speed refrigeration system with an inverter, The Spring Conference of Korean Society of Mechanical Engineering, pp. 2127-2132.

[7] Li Hua, Dong-Woo Lee, Seok-Kwon Jeong, Sam-Sang You, 2006, Decoupling control of variable speed refrigeration system with PI control, International Conference on the Cooling and Heating Technology(Dalian), pp. 564-571.

[8] Dong-Woo Lee, Li Hua, Joo-Ho Yang, Seok-Kwon Jeong, 2006, Fuzzy Control for a Variable Speed Refrigeration System, International

Conference on the Cooling and Heating Technology(Dalian), pp. 572-579.

[9] Li Hua, Seok-Kwon Jeong, 2006, Feedforward control design for a variable speed refrigeration system, Proceeding of 2006 International Symposium on Advanced Engineering(Shanghai), pp. 166-171.

[10] Li Hua, High efficient control design for refrigeration system of a ship, 2006, Autumn Conference of Korean Society of Ocean Engineering, pp. 241-244.

[11] Li Hua, Dong-Woo Lee, Seok-Kwon Jeong, 2006, The superheat and Capacity Control of Variable Speed Refrigeration System with PI Control Logic, The Society of Air-conditioning and Refrigerating Engineering of Korea, pp. 21-26.

[12] Dong-Woo Lee, Li Hua, Seok-Kwon Jeong, Jeong-Pil Choi, 2006, Fuzzy controller design for superheat and capacity control of a variable speed refrigeration system, The Society of Air-conditioning and Refrigerating Engineering of Korea, pp. 27-32.

[13] Li Hua, Dong-Woo Lee, Seok-Kwon Jeong, 2006, PI control design of a variable speed refrigeration system, The Autumn Conference of Korean Society for Power System Engineering, pp. 449-452.

[14] Dong-Woo Lee, Li Hua, Joo-Ho Yang, Seok-Kwon Jeong, 2006, Fuzzy control design of a variable speed refrigeration system for superheat and capacity control, The Autumn Conference of Korean Society for Power System Engineering, pp. 108-113.

[15] Jeong-Pil Choi, Li Hua, Joo-Ho Yang, Seok-Kwon Jeong, 2007, Effective superheat control of variable speed refrigeration system by the smith predictive control, The Spring Conference of Korean Society of Mechanical Engineering, pp. 296-301.

[16] Li Hua, Seok-Kwon Jeong, 2007, Fuzzy control with feedforward compensator for capacity and superheat control of a variable speed refrigeration system, International Conference on the Cooling and Heating Technology(Tokyo), pp. 58-66.

[17] Jeong-Pil Choi, Li Hua, Seok-Kwon Jeong, Joo-Ho Yang, 2007, Design

of PI control with the smith predictive controller for variable speed refrigeration system, International Conference on the Cooling and Heating Technology(Tokyo), pp. 58-66.

[18] Li Hua, Seok-Kwon Jeong, 2007, Independent control of capacity and superheat for a variable speed refrigeration system, The 22nd International Conference of Refrigeration(Beijing), ICR07-E1-1121.

[19] Li Hua, Seok-Kwon Jeong, 2007, Mathematical modeling of a variable speed refrigeration system in state space, The Korean society of heat & cold energy engineers, pp. 114-119.

[20] Jeong-Pil, Li Hua, Seok-Kwon Jeong, Design of predictive controller for effective superheat control of variable speed refrigeration system, The Society of Air-conditioning and Refrigerating Engineering of Korea, pp. 09-15.

Appendix

Appendix A: Padé Approximation program

```
T=100; t_s=1;
t=0:t_s:T;

% 파데 근사법을 이용한 근사
tau2=25;
[np2,dp2]=pade(tau2,1);
GP2=tf(np2,dp2);
G2_1=tf(-0.15,[30,1]);
G2_step=step(G2_1,t);
G2_2=tf(-0.47,[780 1]);

tau3=16;
[np3,dp3]=pade(tau3,1);
GP3=tf(np3,dp3);
G3_1=tf(-0.38, [57 1]);
G3_step=step(G3_1,t);

% 전달함수
G2=G2_2-G2_1*GP2;
y2=step(G2,t);
y2_1=step(G2_2,t);
G3=G3_1*GP3;
y3=step(G3,t);

%지연요소를 갖는 경우
ii2=find(t>tau2);
y2_0=[zeros(ii2(1)-1,1);
G2_step(1:length(ii2))];

ii3=find(t>tau3);
y3_0=[zeros(ii3(1)-1,1);
G3_step(1:length(ii3))];

figure(1)
plot(t,y2_1-y2_0,t,y2,'--')
grid
figure(2)
plot(t,y3_0,t,y3,'--')

syms m
f=0.0171*exp(-0.08*m)-0.0121*exp(-
0.0333*m)+0.006*exp(-0.0013*m);
a=taylor(f,3)
```

Appendix B: Simulation program of decoupling control

```
% 전달함수
G1=tf(-0.42,[680,1]);

tau2_1=25;
[np2_1,dp2_1]=pade(tau2_1,1);
GP2_1=tf(np2_1,dp2_1);
tau2_2=0;
[np2_2,dp2_2]=pade(tau2_2,1);
GP2_2=tf(np2_2,dp2_2);
G2_2=tf(-0.47,[780,1]);
G2_1=tf(-0.15,[30 1]);
G2=G2_2*GP2_2-G2_1*GP2_1;

tau3=16;
[np3,dp3]=pade(tau3,1);
GP3=tf(np3,dp3);
G3_1=tf(-0.38, [57, 1]);
G3=G3_1*GP3;

%상태공간방정식
G1_sys=ss(G1,'min');
[a1,b1,c1,d1]=ssdata(G1_sys);

G2_sys=ss(G2,'min');
[a2,b2,c2,d2]=ssdata(G2_sys);

G3_sys=ss(G3,'min');
[a3,b3,c3,d3]=ssdata(G3_sys);

%초기설정
Ta_ref=5333; Ta_out=5440;
SH_out_1=160;
% Ta_ref=5387; Ta_out=5440;
   SH_out_1=160;
% Ta_ref=5333; Ta_out=5387;
   SH_out_1=122;
SH_ref=160;SH_out=160;

x1=0;x2=0;x3=0;
u1_I=0;u1_PI=0;
u2_I=0;u2_PI=0;
u1_0=10100;u1_1=u1_0;u1_2=u1_0;
%u1_0=11352;u1_1=u1_0;u1_2=u1_0;
u2_0=12800;u2_1=u2_0;u2_2=u2_0;
%u2_0=11625;u2_1=u2_0;u2_2=u2_0;
u_1=0;u_2=0;sh=0;

% 제어기
Kp_1=800;Ki_1=0.2;K1=0;
Kp_2=12;Ki_2=0.25;K2=0;

%시뮬레이션 설정
T_all=30*40;
T_Ta=30;T_SH=15;
T_control=0.1;T_model=0.01;
n_Ta=T_all/T_Ta;
n_SH=T_all/T_SH;

y0_1=zeros(n_Ta,1);
y1_1=y0_1;y1_2=y0_1;
y1_3=y0_1;y1_4=y0_1;
y0_1=T_Ta:T_Ta:T_all;

y0_2=zeros(n_SH,1);
y2_1=y0_2;y2_2=y0_2;y2_3=y0_2;
y0_2=T_SH:T_SH:T_all;

% 용량제어
for s1=1:1:n_Ta

if u1_0>16000
   u1=16000;
elseif u1_0<8000
    u1=8000;
else u1=u1_0;
end
```

```
if SH_out_1<0
SH_out_1=0;
end

u_1=(u1-u1_1)*60/16000;
u1_1=u1;
y1_4(s1,1)=u_1;

for s1_1=1:1:T_Ta/T_control

delta_Ta=Ta_out-Ta_ref;
u1_I=u1_I+delta_Ta*T_control;
u1_PI=Kp_1*delta_Ta+Ki_1*u1_I;
u1_0=u1_2+u1_PI;

for s1_2=1:1:T_control/T_model

x1_dot=a1*x1+b1*[u_1 0];
x1=x1+x1_dot*T_model;
y1=c1*x1;

x2_dot=a2*x2+b2*[u_1 0 0];
x2=x2+x2_dot*T_model;
y2=c2*x2;

end

Ta_out=Ta_out+y1(1,1)*16000/600;
SH_out_1=SH_out_1+y2(1,1)*16000/600;
u_1=0;

end

y1_1(s1,1)=Ta_out*600/16000-200;
y1_2(s1,1)=SH_out_1*600/16000;
y1_3(s1,1)=u1*60/16000;

end

% 과열도 제어
for s2=1:1:n_SH

k=round(s2/2);
u_3=y1_4(k,1);

if u2_0>16000
   u2=16000;
elseif u2_0<1600
   u2=1600;
else u2=u2_0;

end

u_2=(u2-u2_1)*100/16000;
u2_1=u2;

for s2_1=1:1:T_SH/T_control

delta_SH=SH_out-SH_ref;
u2_I=u2_I+delta_SH*T_control;
u2_PI=Kp_2*delta_SH+Ki_2*u2_I;
u2_0=u2_2+u2_PI;

s1_2=1:1:T_control/T_model

x2_dot=a2*x2+b2*[u_3 0 0];
x2=x2+x2_dot*T_model;
y2=c2*x2;

x3_dot=a3*x3+b3*[u_2 0];
x3=x3+x3_dot*T_model;
y3=c3*x3;

end

SH_out=SH_out+(y2(1,1)+y3(1,1))*16000
/600;
u_3=0;u_2=0;

end

y2_1(s2,1)=SH_out*600/16000;
```

```
y2_2(s2,1)=u2*100/16000;
u2_0=u2_0+(y1_2(k,1)/0.45)*16000/100;
end

figure(1)
subplot(2,1,1)
plot(y0_1,y1_1)
axis([0,1400,-2, 10]);
grid

subplot(2,1,2)
plot(y0_1,y1_3)
axis([0,1400,30, 70]);
grid
figure(2)
subplot(2,1,1)
plot(y0_2,y2_1)
axis([0,1400,0, 10]);
grid
subplot(2,1,2)
plot(y0_2,y2_2)
axis([0,1400,50, 100]);
grid
```

Appendix C: PLC program of PI control

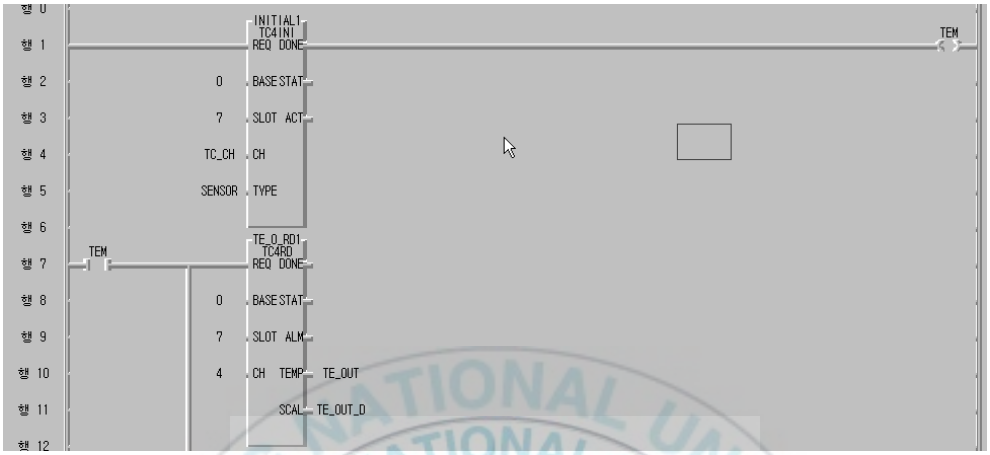

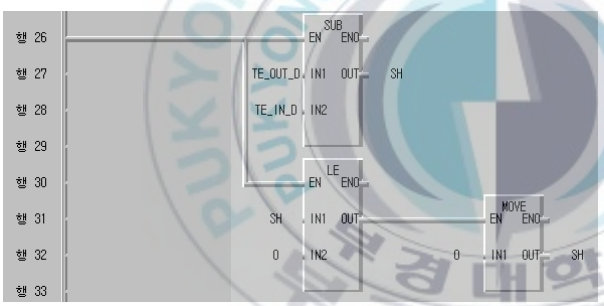

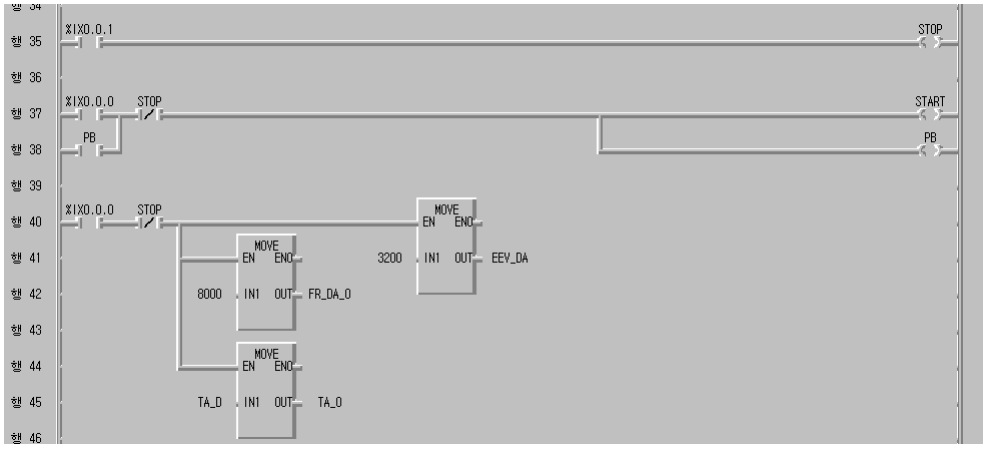

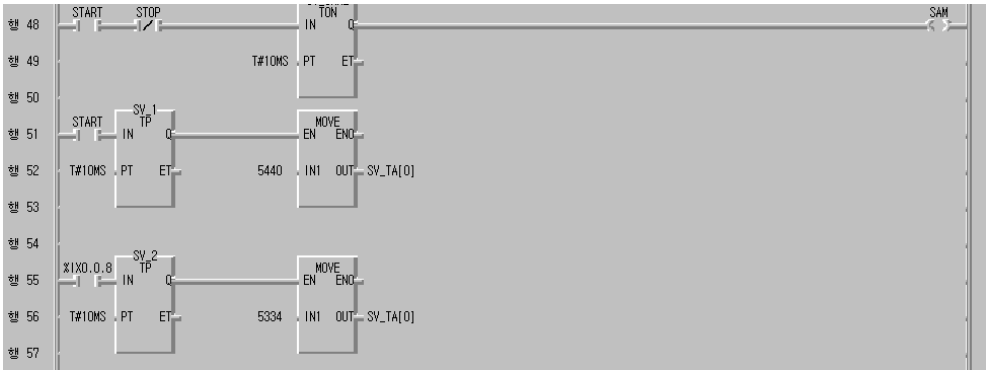
START
STOP
TON
IN Q
SAM
T#10MS PT ET
SV_1
TP
MOVE
EN ENO
5440 IN1 OUT SV_TA[0]
SV_2
%IX0.0.8
5334
SV_TA[0]

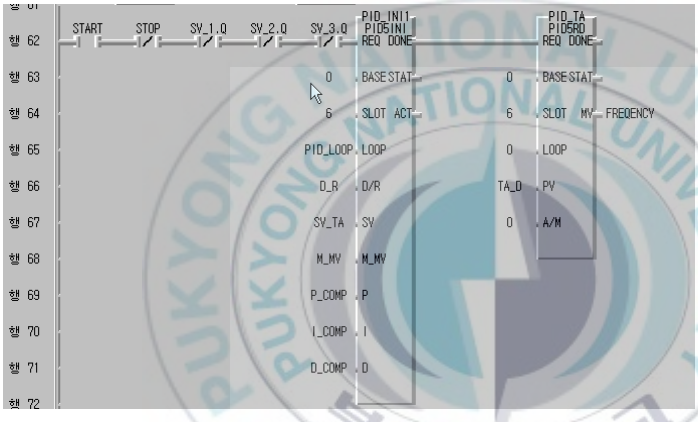
START
STOP
SV_1.Q
SV_2.Q
SV_3.Q
PID_INIT
PID5INI
REQ DONE
PID_TA
PID5RD
BASESTAT
SLOT ACT
MV FREQENCY
LOOP
D/R
SV
M_MV
P_COMP
I_COMP
D_COMP
PV
A/M

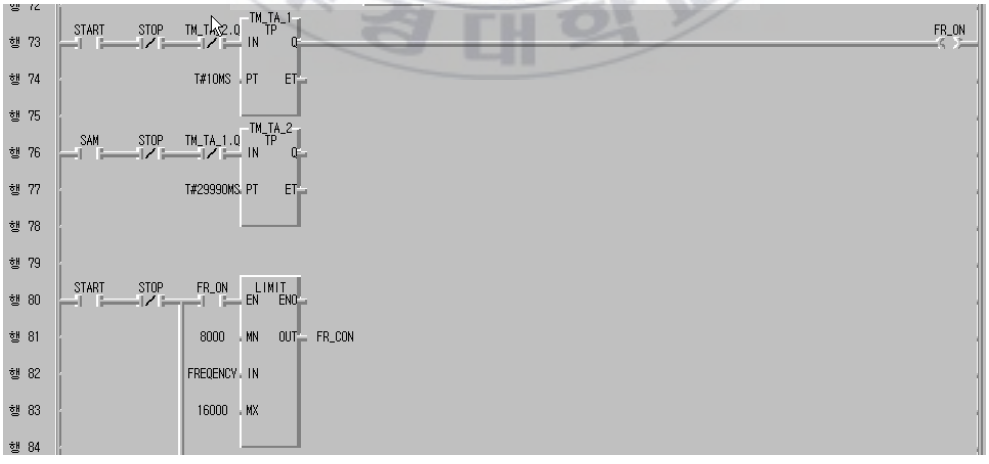
START
STOP
TM_TA_1.Q
TM_TA_1
TP
IN Q
FR_ON
T#10MS PT ET
SAM
TM_TA_2
T#29990MS
LIMIT
EN ENO
8000 MN OUT FR_CON
FREQENCY IN
16000 MX

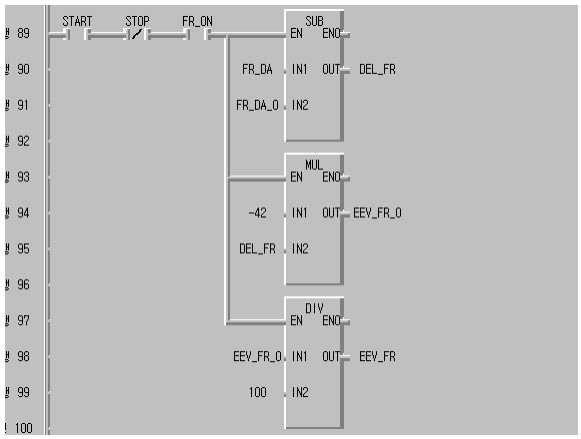
START
STOP
FR_ON
SUB
EN ENO
FR_DA
IN1 OUT
DEL_FR
FR_DA_0
IN2
MUL
-42
EEV_FR_0
DEL_FR
DIV
100
EEV_FR

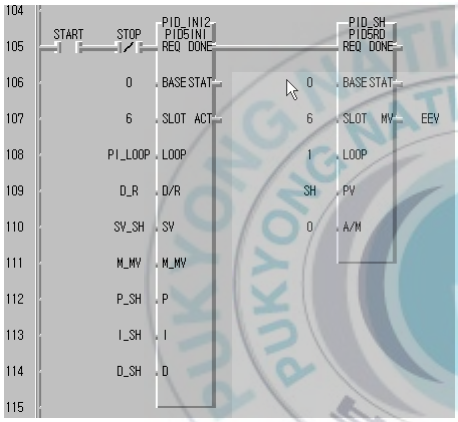
START
STOP
PID_INI2
PID5INI
REQ DONE
PID_SH
PID5RD
BASESTAT
SLOT ACT
LOOP
D/R
SV
M_MV
P
I
D
SLOT MV
EEV
PV
A/M
PI_LOOP
SV_SH
P_SH
I_SH
D_SH

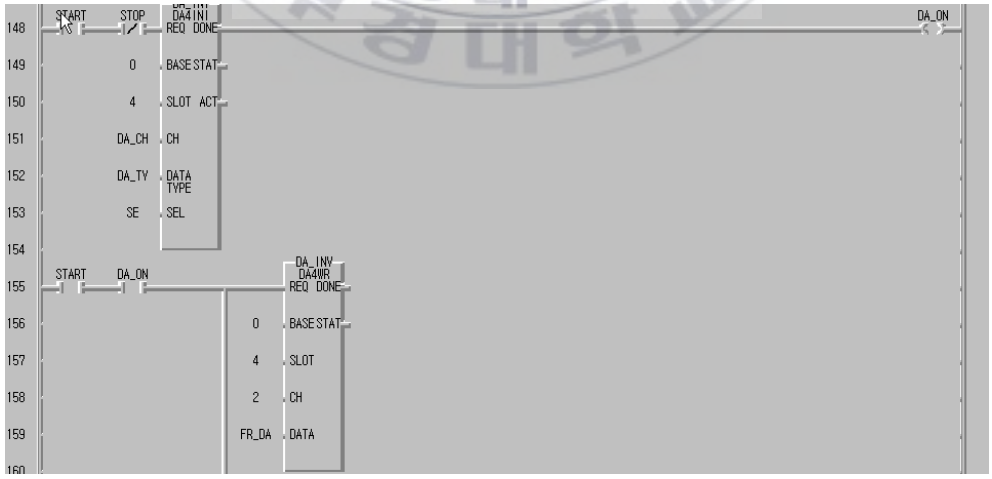
START
STOP
DA4INI
REQ DONE
DA_ON
BASESTAT
SLOT ACT
CH
DATA TYPE
SEL
DA_CH
DA_TY
SE
START
DA_ON
DA_INV
DA4WR
REQ DONE
BASESTAT
SLOT
CH
DATA
FR_DA

Appendix D: PLC program of fuzzy control

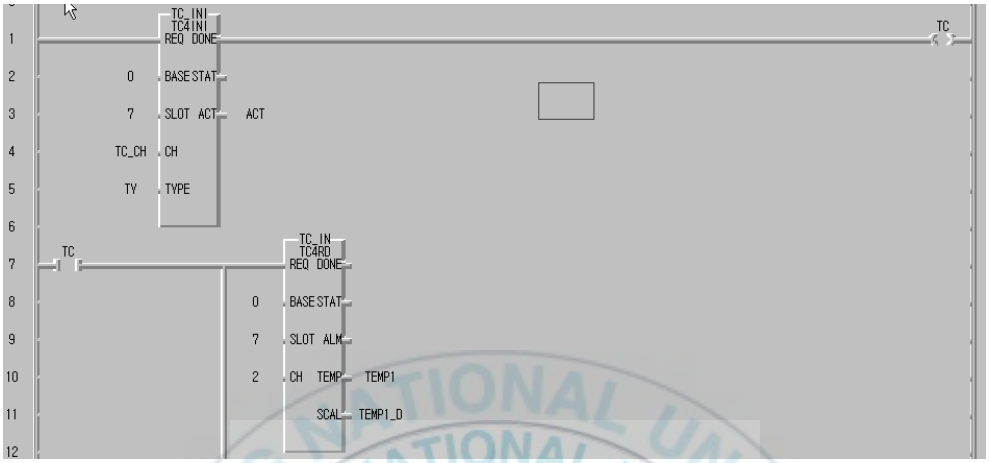

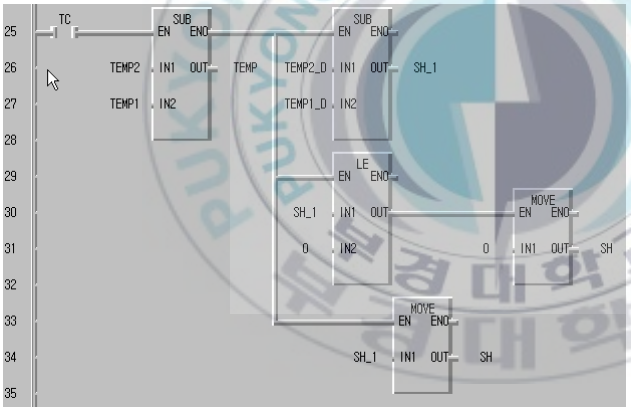

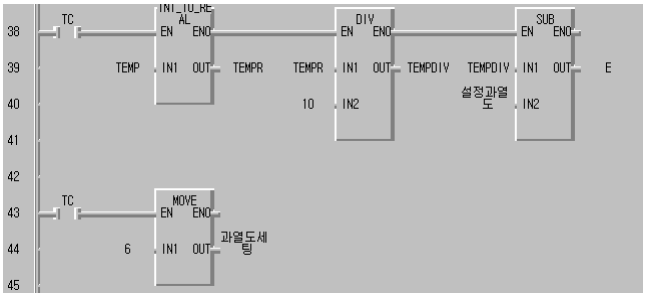

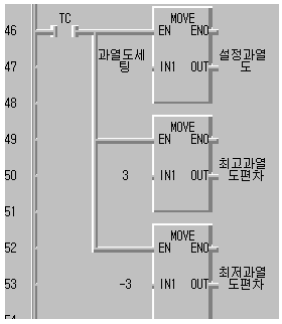
TC
MOVE
EN ENO
과열도세팅
IN1 OUT
설정과열도
MOVE
EN ENO
3
IN1 OUT
최고과열도편차
MOVE
EN ENO
-3
IN1 OUT
최저과열도편차

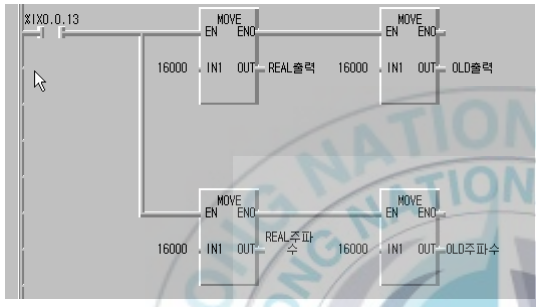
%IX0.0.13
MOVE
EN ENO
16000
IN1 OUT
REAL출력
MOVE
EN ENO
16000
IN1 OUT
OLD출력
MOVE
EN ENO
16000
IN1 OUT
REAL주파수
MOVE
EN ENO
16000
IN1 OUT
OLD주파수

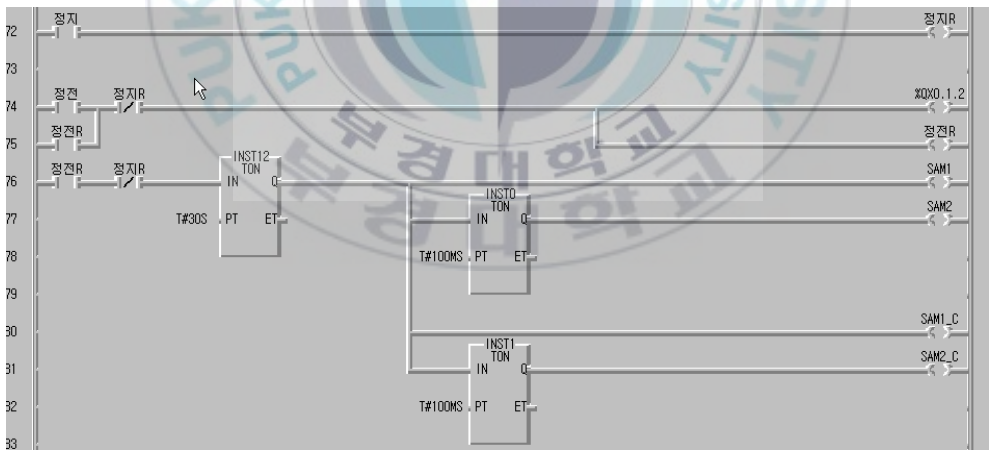
정지
정지R
정전
정지R
%QX0.1.2
정전R
정전R
정지R
INST12
TON
IN Q
SAM1
T#30S
PT ET
INST0
TON
IN Q
SAM2
T#100MS
PT ET
SAM1_C
INST1
TON
IN Q
SAM2_C
T#100MS
PT ET


SAM1
INST3.Q
INST2
TP
IN Q
양자화
T#100MS
PT ET
SAM2
INST2.Q
INST3
TP
IN Q
T#30S
PT ET

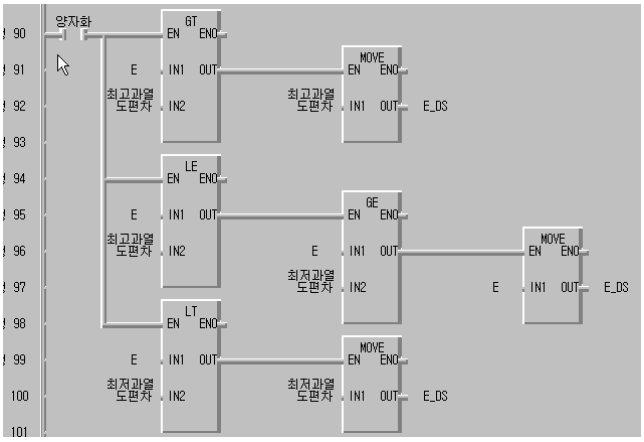
양자화
GT
EN ENO
E
IN1 OUT
최고과열 도편차
IN2
MOVE
EN ENO
최고과열 도편차
IN1 OUT
E_DS
LE
GE
LT
최저과열 도편차

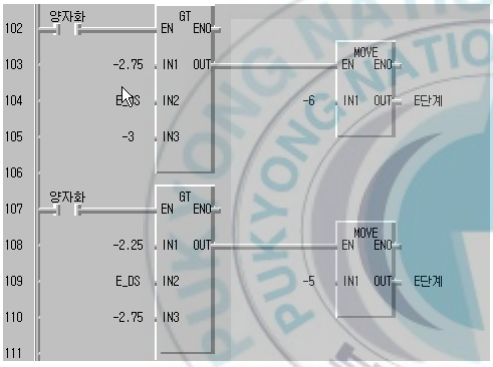
양자화
GT
EN ENO
-2.75
IN1 OUT
E_DS
IN2
-3
IN3
MOVE
-6
E단계
-2.25
-5

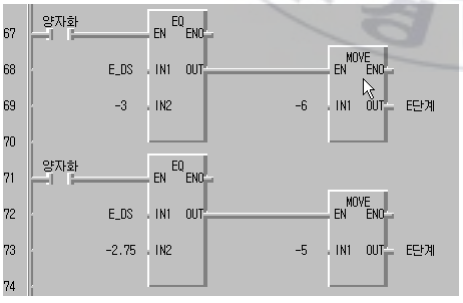
양자화
EQ
EN ENO
E_DS
IN1 OUT
-3
IN2
MOVE
-6
E단계
-2.75
-5

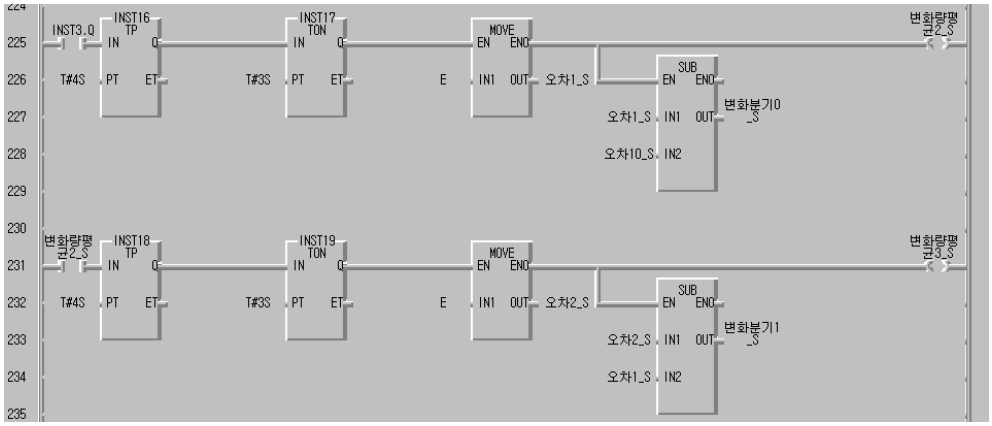
INST3.Q
INST16
TP
T#4S
INST17
TON
T#3S
MOVE
E
오차1_S
SUB
오차1_S
오차10_S
변화분기0_S
변화량평균2_S
INST18
INST19
오차2_S
변화분기1_S


변화평균계산_S
ADD
변화분기0_S
변화분기1_S
변화분기2_S
변화분기3_S
변화분기4_S
변화분기합0_S
변화분기5_S
변화분기6_S
변화분기7_S
변화분기8_S
변화분기9_S
변화분기합_S


변화평균계산_S
DIV
변화분기합_S
30
E변화량
필터_S

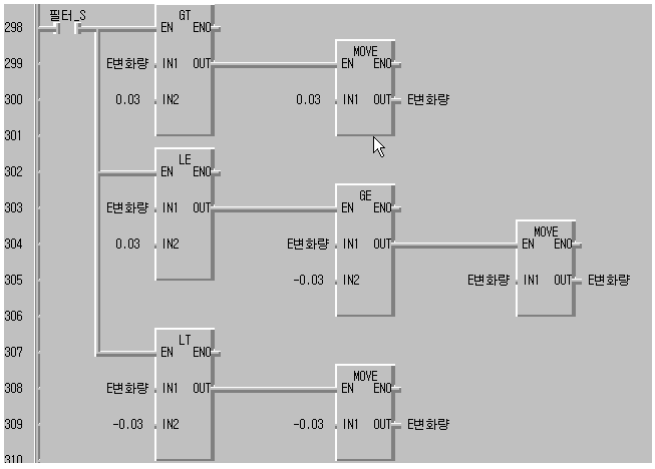
필터_S
GT
E변화량
0.03
MOVE
LE
GE
-0.03
LT

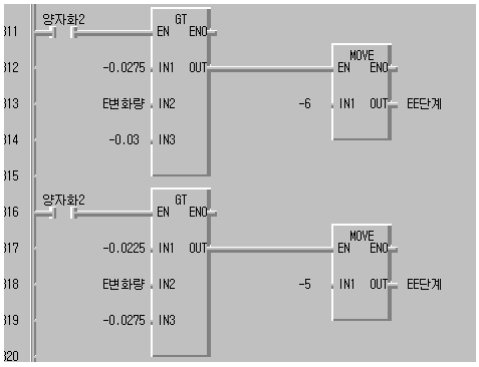
양자화2
GT
-0.0275
E변화량
-0.03
MOVE
-6
EE단계
양자화2
GT
-0.0225
E변화량
-0.0275
MOVE
-5
EE단계

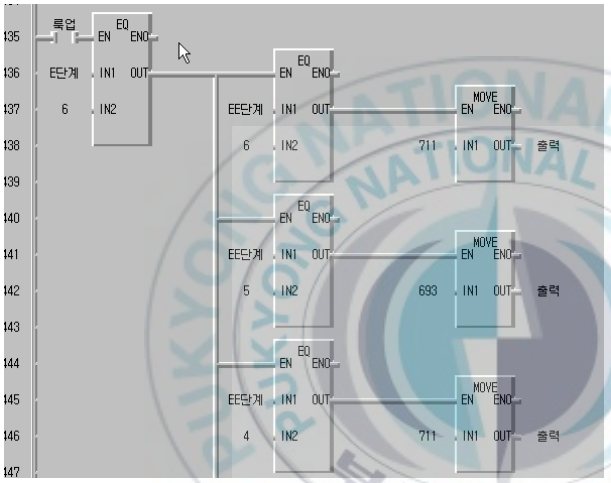
룩업
EQ
E단계
6
EE단계
6
711
출력
EE단계
5
693
출력
EE단계
4
711
출력

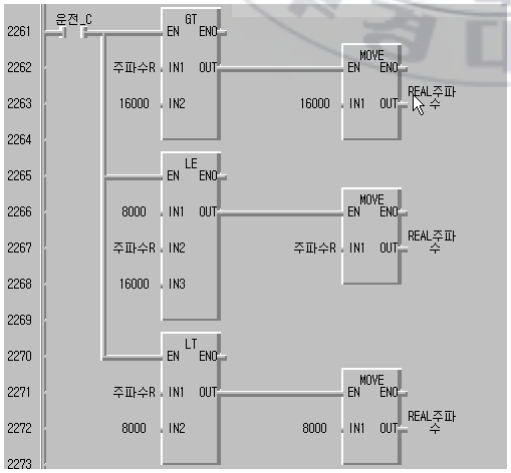
운전_C
GT
주파수R
16000
16000
REAL주파수
LE
8000
주파수R
16000
주파수R
REAL주파수
LT
주파수R
8000
8000
REAL주파수

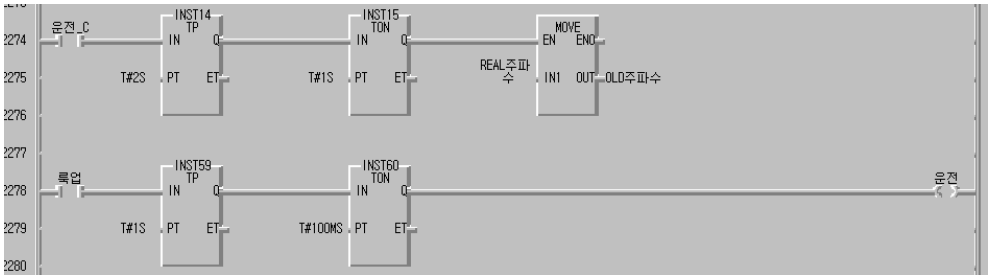
운전_C
INST14
TP
IN
Q
T#2S
PT
ET
INST15
TON
IN
Q
T#1S
PT
ET
MOVE
EN
ENO
REAL주파수
IN1
OUT
OLD주파수
룩업
INST59
TP
IN
Q
T#1S
PT
ET
INST60
TON
IN
Q
T#100MS
PT
ET
운전

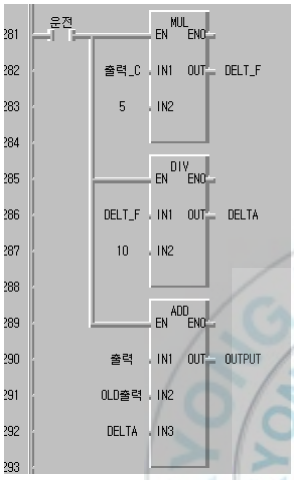
운전
MUL
EN
ENO
출력_C
IN1
OUT
DELT_F
5
IN2
DIV
DELT_F
IN1
OUT
DELTA
10
IN2
ADD
출력
IN1
OUT
OUTPUT
OLD출력
IN2
DELTA
IN3

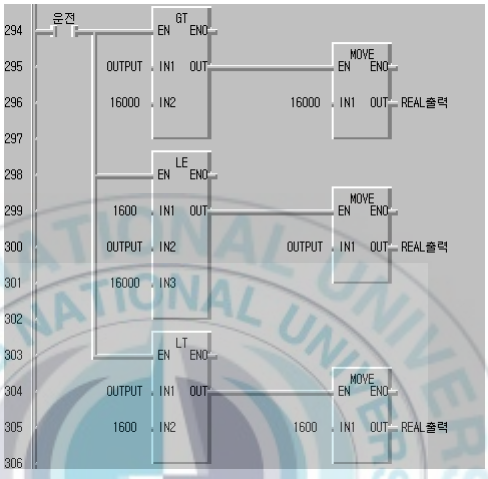
운전
GT
EN
ENO
OUTPUT
IN1
OUT
16000
IN2
MOVE
16000
REAL출력
LE
1600
OUTPUT
IN3
LT


정전R
DA_INI2
DA4INI
REQ
DONE
DA
0
BASESTAT
4
SLOT
ACT
채널
CH
DATA
DATA TYPE
SEL
SH_IN2
DA4WR
7
REAL출력

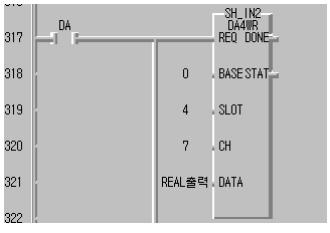
DA
SH_IN2
DA4WR
REQ
DONE
0
BASESTAT
4
SLOT
7
CH
REAL출력
DATA

Acknowledgements

5년 동안의 한국 유학생활을 마무리하면서 아쉬움도 많고 즐거웠던 점도 많지만, 무엇보다도 내 인생에서 되돌릴 수 없는 소중한 시간이었다고 생각합니다. 특히 AMCL에서 보낸 시간들은 저에게 잊을 수 없는 추억으로 남게 될 것입니다.

부족한 논문이 완성되기까지 저에게 아낌없는 지도와 격려를 해주시고, 유학생활의 어려움을 참아낼 수 있게 항상 사랑으로 감싸주신 정석권 교수님께 진심으로 감사드립니다. 교수님께서는 저한테 학문만 가르치신 것이 아니라 학문을 연구하는 연구자로써의 도리를 깨우쳐 주셨으며 진정한 인간이 되도록 이끌어 주셨습니다. 또한, 항상 묵묵히 AMCL에 지원을 아끼시지 않으시는 사모님께도 감사의 말씀을 올립니다. 제자를 사랑하시는 마음으로 항상 관심을 가져주시고 논문의 주심을 맡아주신 윤정인 교수님, 그리고 항상 가까이에서 관심과 배려로 힘이 되어주고 논문의 심사위원을 맡아주신 금종수 교수님, 김종수 교수님께 감사드립니다. 그리고 논문의 완성을 위해서 많은 조언을 해주시고 좋은 결실을 맺도록 귀중한 시간을 내주셔 논문의 영문 수정을 해주시고 심사위원까지 맡아주신 한국해양대학 기계정보공학부의 유삼상 교수님께도 진심으로 감사드립니다.

한국 유학생활이 평탄한 배움의 길은 아니었지만 저를 AMCL과 인연을 맺게 해주고 생활뿐만 아니라 학문에도 많은 도움을 준 중국 연산대학의 이진국 박사께 진심으로 감사를 드립니다. AMCL의 첫 냉동과 대학원생으로서 혼자 고독한 연구를 하고 있을 때 연구실에 들어와 함께 연구를 해왔던 이동우와 윤종수 후배님, 항상 AMCL에 활기를 더해주고 저를 웃게 해준 이동규 후배님, 그리고 반년간 혼자서 연구실의 일을 도맡아 해온 최정필 후배님께 진심으로 감사드립니다. 학업에 대한 열정으로 메카트록닉스협동과정에 입학해서 AMCL의 맴버가 되신 정태영, 김종백 선배님, 다음 학기에 대학원에 진학하여 AMCL의 기둥이 되실 변종영 후배님, 남은 대학원 생활을 학문에 매진하셔서 좋은 연구성과 얻기를 기

원합니다. 그리고 연구실에서 열심히 공부하고 있는 안성훈, 안성현, 조건붕 후배님, 취업을 하셔서 열심히 일하고 계시는 최봉석 씨, 김성하 씨, 안세진 군, 한유빈 양 외 AMCL에 몸담았었던 모든 이들에게 깊은 고마움을 전하면서 앞날에 무궁한 발전이 있기를 기원합니다.

5년간 부경대학에서 유학생활을 하면서 희로애락을 함께 해온 큰 언니 같았던 대련수산대학의 이화 교수님, 힘든 유학생활 동안 가족처럼 서로 힘이 되어 주었고 항상 도움과 관심을 주신 중국 강소기술사범대학의 지용수 교수님, 중국 석유대학의 장만송 교수님, 임춘단 교수님, 중국 상해수산대학의 허철 교수님, 학회의 인연으로 만나서 변함없는 도움과 관심을 주신 중국 대련이공대학의 沈胜强 교수님께 진심으로 감사를 드립니다. 학업을 마치고 한국에서 근무하고 있는 박영일 씨, 리리 양, 이미화 양, 졸업을 앞둔 고의가 양, 왕호강 군, 장빈 군에게도 깊은 고마움을 전하면서 무궁한 발전이 있기를 기원합니다. 그리고 지금도 부경대학에서 열심히 연구를 하고 계시는 환경지질학과 엄결 씨, 화학과 천충길 씨, 기계공학부의 채용길 군, 귀여운 동생 이연 양을 비롯한 모든 중국 유학생들이 학업에 매진하여 좋은 결실 맺기를 기원합니다.

끝으로, 그 동안 묵묵히 절 지켜주시고 걱정해주신 부모님, 그리고 늘 격려해주던 동생 부부와 사랑스러운 조카, 모든 가족과 친지 분들께 이 작은 결실과 영광을 바칩니다.

2008년 7월 李 花 拜上